CHALMERS

The mechanical point impedance
of the skin-penetrated human skull in vivo
Master of Science Thesis in Biomedical Engineering

FAUSTO WOELFLIN

Department of Signals and systems
Biomedical signals and systems division
CHALMERS UNIVERSITY OF TECHNOLOGY
Göteborg, Sweden, 2011
Report No. EX050/2011

Title: The mechanical point impedance of the skin-penetrated human skull in vivo

Report No. EX050/2011

Chalmers Institute of Technology

Göteborg, Sweden, 2011

Department of Signals and Systems
Biomedical Signals and Systems

Abstract

The mechanical point impedance of the human skull is an important patient property to consider in the design of both transducers for bone-anchored hearing aids (baha) and artificial test devices for the baha. This property has also a scientific value for the understanding of the transmission mechanics in hearing by bone conduction.

In this study the mechanical point impedance of the percutaneous implant for attachment of a baha was investigated on 47 human subjects from Sweden and Canada. A swept sine from 100 to 10k Hz was used to drive a transducer attached to the backside of a B&K impedance head, coupled to the implants with the snap coupling used by the present manufacturers of the baha (Cochlear and Oticon Medical). In five of the subjects, who had bilateral implants, the transfer function between the implants of both sides (transcranial accelerance) was also investigated. In a separate study the mechanical characteristics of the snap couplings used by two manufacturers of the baha was compared.

It was found that the mechanical point impedance in all subjects is characterized by a more or less pronounced anti resonance (peak) in the range of 100-200 Hz. Above this anti resonance the mechanical impedance is mainly negatively sloping and hence compliance (inverse to stiffness) controlled. Generally this characteristic is not significantly different from what is presented in previous studies but in this study impedance parameters are also analyzed for specific patient properties such as gender, undergone surgeries and age.

From the study of the two different snap couplings it was found that the compliance of the Oticon coupling (187n m/N) was 15 % softer than the compliance of the Cochlear coupling (163n m/N). This difference in compliances may not be of clinical importance as both couplings are stiffer than what is seen in the impedance of the subjects (400n m/N at 1 kHz).

In view of the large sample size the parameters extracted from the impedance data in this study will give a reliable estimate of the "normal adult" skull impedance seen at the typical implant site for baha devices. Future work should focus on the in-situ mechanical point impedance of pediatric patients.

Keywords
bone conduction, titanium implant, mechanical point impedance, transcranial transfer function, baha, bone-anchored hearing aid, snap coupling, cochlear, oticon.

List of abbreviations

MPI: mechanical point impedance
baha: bone anchored hearing aid
dBHL: decibel hearing loss
RMS: root mean square
CSV: Comma-separated values
iRSM: Institute for Reconstructive Sciences in Medicine

Acknowledgements

The chances of you holding these pages in your hands were once so remotely small that one wouldn't be too wrong guessing it was simply not possible. There is not enough room in this page to list the many bureaucratic, cultural and economic barriers that, depending strongly on the geographical birthplace, a person may encounter between his present and his goals.

The difference between this and some other story is that I was lucky enough to have as many hurdles as people helping me out along the way. Their efforts and good hearts are the ones that made it possible for a young, middle-class man from Argentina without money or influences, to achieve a Master of Science degree in the best technical university in Sweden.

Thanks to my examiner Bo Håkansson for generously transmitting so much of your enthusiasm, curiosity and experience to me, and for trusting me for this project.

Thanks Bill Hodgetts for the chance, and for the hours of interdisciplinary debates both in person as well as through internet.

Thanks Dylan Scott and Herman Lundgren for all the help during the very fun experimental stages of this work.

Thanks Anders Tjellström for your patient explanations of the different surgical procedures, and your help with the Swedish patients.

Thanks Ulla Blomqvist for the trust and help provided during the initial phases of this journey.

Thanks Lena Berg for aiding me when pursuing every new and unconventional academic goal.

Thanks to my Swedish parents Vannie and Göran Gezelius, for reshaping my life and my future with your unconditional love and care.

Thanks to my Argentinean parents Felix I. Woelflin and Nora P. Sesso for intentionally providing me with the tools necessary to grow in this, and every other aspect of my life.

Thanks to my siblings Exequiel, Tomas and Eloisa for your constant support, and for filling my life with joy.

Last, but definitely not least, I would like to thank my life's companion and my girlfriend Mariela Martin: Your unselfish and constant love kept me going and made every step worthwhile and possible.

Contents

1.   Introduction

Hearing impairment is a type of disability that currently affects more than 278 million people worldwide (WHO, 2010). This type of affliction can be congenital or acquired, and affect the organs involved in different degrees. Major causes of acquired hearing impairment are infectious diseases such as meningitis, measles, mumps and chronic ear infections. Other common causes include exposure to excessive noise, traumatic head and ear injury and ageing.

The quality of life of many of these patients could be significantly improved by the used of different kinds of hearing aids depending on their pathology. Bone anchored hearing aids (abbreviated "baha") are devices that take advantage of the principle of direct bone conduction, to transmit sound via skull bone vibration from the surroundings to the patient's healthy cochlea. This is particularly important for patients with conductive hearing loss, as it provides with a way to bypass the outer- and middle ear which are of vital importance in air-conducted sound transmission. The baha system consists in a surgically implanted percutaneous titanium fixture (Brånemark et al., 1977) on the mastoid portion of the temporal bone, and an external sound processor that converts sound pressure waves to mechanical stimulation.

The following is a short explanation intended to provide the reader with useful theoretical tools to understand the importance of bone anchored hearing aids and the present study.

2.   Background

Anatomy and mechanics of hearing

The ear is the primary sensing organ for sound and can be divided in three main parts: the outer-, middle- and inner ear. The outer ear consists of the external cartilage and skin, and the auditory canal. Its function is to filter, reflect, and transmit sound to the middle ear. The middle ear contains three bones known as ossicles, in an air-filled cavity that connects the eardrum and the cochlea. The ossicles act as amplifying mechanical levers that transmit the vibration of the tympanic membrane to what is known as the oval window; a membrane that separates the middle ear from cochlea. The cochlea contains the sensory organ of the inner ear. The vibrations propagated through the fluid contained in the cochlea, stimulate the hair cells of the organ of Corti; a biological transducer that converts the mechanical vibrations in the frequency range of 20 Hz to 20 kHz, to action potentials in its hair cells. These electrical impulses are transmitted via the auditory nerve to the brain for interpretation.

The main mechanism of stimulation of inner- and outer hair cells follows the air-conduction path: sound pressure waves are conducted from the surroundings, through the outer ear to the ear drum. The ossicles amplify and transmit these longitudinal waves to the oval window. This sets fluid in the cochlea in movement, which excites the hair cells.

However, there is another path that vibrations can take in order to finally excite the organ of corti so that a person can sense sound: the bone-conduction path. The inner ear is contained and surrounded by skull bone. Vibrations that make the skull bone oscillate put the inner ear in movement too. The fluid inside the cochlea moves in a similar manner to what air-conducted vibrations can generate, thus, action potentials are generated by inner- and outer hair cells which ultimately can be interpreted by the brain as sound.

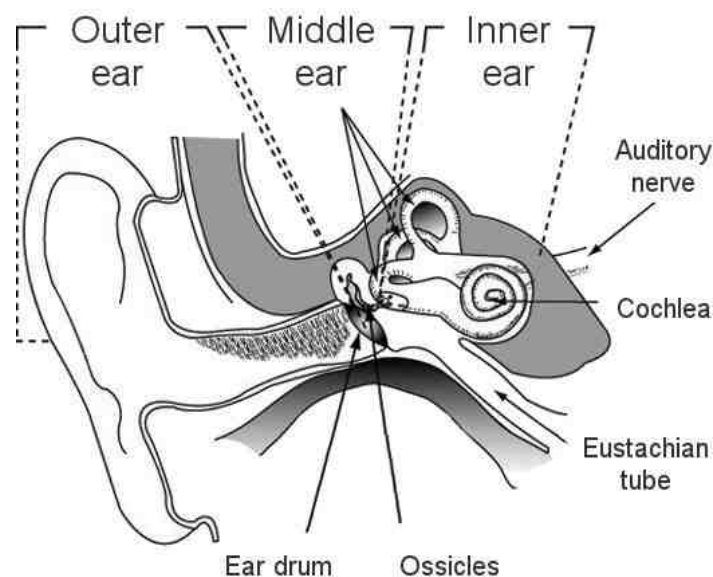Air conduction is the main path for sound from the surroundings to be interpreted by a person. For

Figure 1 Drawing of the human ear

sound from a person's own voice, however, there is a big contribution of the bone-conduction path. This is the reason why people seldom recognize their own voice when listening to it from a recording: they are used to hear it mainly through the mechanisms of bone-conduction, which aren't activated when listening to the longitudinal air waves generated by a speaker.

Bone conduction amplification devices

As stated before, a healthy person will pick up most sound pressure waves from its surroundings by air-conduction mechanisms. These mechanisms require healthy outer- and middle ears to function properly; problems with any of them may result in impaired hearing in that side of a person's head.

Hearing impaired patients with healthy inner ears can be aided by bone conduction amplification devices. These are electro-mechanical devices that provide the patient with a way of bypassing the outer and middle ear to finally stimulate the healthy cochlea. This work is mainly related to the bone-anchored hearing aid.

Previous hearing aids based in bone conduction, but without skin penetrating implants, had to deal with the attenuating effect of the skin as well as with frequent irritation of this tissue because of the pressure needed on the device to effectively transmit vibration. Titanium implants with specific surface treatment, on the contrary, allow bone cells to grow and develop closely in a process called osseointegration (Albrektsson et al., 1983), which gives a solid support for the external sound controller. The mechanical connection between the implant abutment and the sound controller is made through a plastic snap coupling.

The baha was the result of a project that started in the late seventies in Göteborg, Sweden. It was carried out in collaboration between the Department of Applied Electronics of Chalmers University of Technology, the ENT-department of Sahlgrenska Hospital, the Department of Audiology from University of Göteborg, and the Institute for Applied Biotechnology.

3.   Aim of this study

To understand and improve this method of bone stimulation it is important to study how the system works, and the properties that govern its behavior. One of those properties is the mechanical point impedance (MPI) of the implant-skull system. The MPI is a measure of how much the bone structure resists motion when subjected to a force stimulation of a given amplitude and frequency by the baha.

The output impedance of the transducers used for bahas is orders of magnitude smaller than the input impedance of the human skull seen at the implant's site. This mismatch results in small intersubject variability in force output from the transducer. When the titanium screw is implanted closer to the ear canal instead, where the skull impedance magnitude is much higher, there is an increase in hearing sensitivity as well which cannot be explained from force output variations. This means that a relationship is likely to exist between hearing sensitivity and impedance. The main scope of this study is then, to accurately measure and determine the mean patient's skull impedance seen at the baha implant's site (55 mm posterior and anterior to the ear canal opening.

Most previous studies of mechanical point impedance of the human skull were made on cadavers or dry skulls. In 1986, Håkansson conducted a study on seven living subjects, but the abutment-coupling pair used back then was very sensitive to connection-angle variations (Håkansson et al., 1986). Nowadays, there are more robust design concepts of the abutment-coupling pair, which leads to a more standardized measurement procedure. This, in turn, can lead to a more reliable generalization of the measurement results.

Being the scope for the present study, to gain understanding that may directly be applicable to improve assisted bone-conduction hearing; the measurement procedure contemplates the frequency band between 100 Hz and 10 kHz. The results presented in this study are based on measurements made on forty five living human subjects with titanium implants for baha. The first seven patients were measured in Göteborg, Sweden. The resting thirty eight were measured in the city of Edmonton, Alberta, Canada.

Some of the measured patients had bilateral implants, that meaning that they used bahas on both sides of the head. On five of these subjects, the transfer accelerance function of the vibrations from one of the implants to the implant on the contralateral side was also studied. This was the second goal of the present investigative work.

A third objective is to compare the mechanical properties of the plastic snap couplings used to secure the baha's sound controller to the implant abutment, which has never been studied before. The two biggest manufacturers of bone-anchored hearing aids use slightly different design approaches. The aim of this part of the study was to try to find similarities and differences in their capability of transmitting mechanical stimulus from the sound controller's transducer to the skull, throughout the measured frequency band.

The fourth goal of the present study, but one of the first ones to be achieved chronologically speaking, was to design, program and build a complete MPI measurement setup at the Interfacial Biomechanics Laboratory of the Institute for Reconstructive Sciences in Medicine of Canada.

4.   Methods and apparatus

The definition of mechanical point impedance Z used in this work is the quotient between the excitation force F from the transducer and the response velocity v from the implant's abutment:

$$Z = \frac{F}{v} \qquad (1)$$

As named earlier in this work, the mechanical impedance of a structure is its resistance to motion velocity when an exciting force of a certain magnitude and frequency is applied. A high value for the magnitude of the impedance means small vibrations in the skull for that given force, and vice versa.

Forty five living human subjects with titanium fixtures for bone-anchored hearing aids were studied. Their date of birth, gender and a measured side are presented in table 5 in the appendix. The whole patient database isn't shown because of its size. Other important patient parameters included in the full version of the database were: undergone surgeries for each side of the head, type of patient (unilateral or bilateral), known pathologies or syndromes at the time of measurement.

The equipment used for measurement setup is presented in table 1:

Table 1 – equipment used for measurement setups

| Equipment name	Brand & model / Type	Note
Signal Analyzer	Agilent 35670A	Used for measurements in Sweden
Data cquisition system	NI-cDAQ 9172	Used for measurements in Canada
Impedance head	Brüel & Kjær 8001	Used for measurements in Sweden and Canada
IPC accelerometer	--	Used for measurements in Sweden
IPC accelerometer	Dytran	Used for measurements in Canada
Charge amplifier	Brüel & Kjær 2635	Connected to the "Force" output of the impedance head in Sweden
Charge amplifier	Brüel & Kjær 2651	Connected to the "Acceleration" output of the impedance head in Sweden
Charge-to-deltaTron amplifier	Brüel & Kjær 2647	Connected to the "Force" output of the impedance head in Canada
Charge-to-deltaTron amplifier	Brüel & Kjær 2647	Connected to the "Acceleration" output of the impedance head in Canada
Transducer	BEST	Used for measurements in Sweden and Canada
GPIB - USB interface	NI	Used to connect the Agilent signal analyzer to the computer
Custom thread adapter	Male 10-32 to female M2	Used to connect the impedance head to the different snap couplings
Custom thread adapter	Flat surface female M2	Used to connect the IPC accelerometer to the Cochlear snap coupling
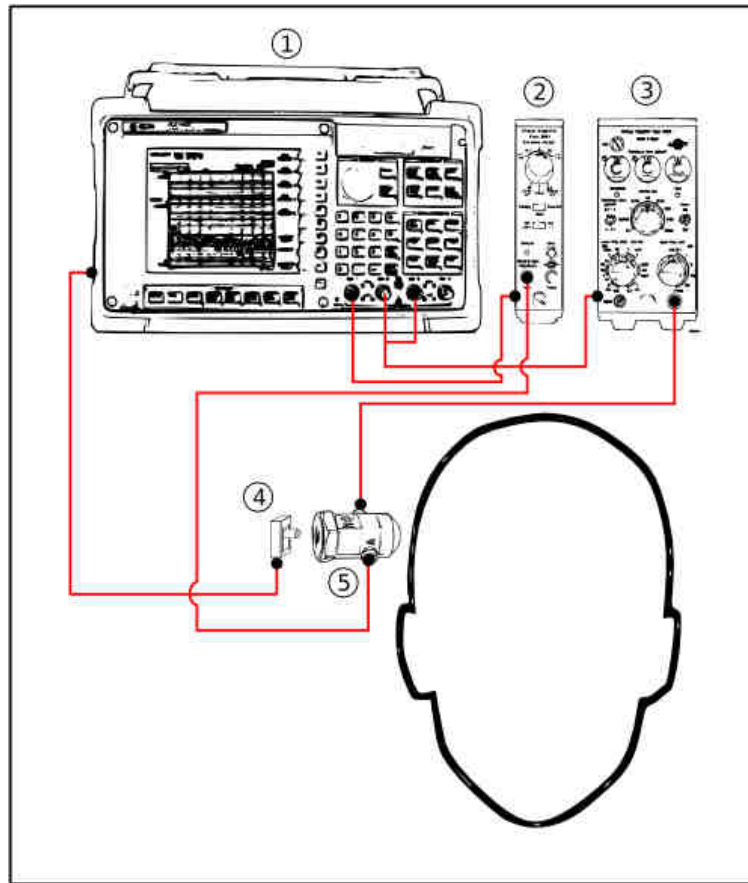
Figure 2 - Setup used for MPI measurements in Göteborg, Sweden.
1- Agilent 35670A signal analyzer, 2- B&K 2635 charge amp, 3- B&K 2651 charge amp, 4- BEST transducer, 5- B&K 8001 impedance head.

Notice that some of the equipment used to measure the Canadian patients differs from that used in Sweden but both set-ups were later proved to be equivalent. In Canada, the signal analyzer was replaced by a PC running LabView™ from NationalInstruments, and a USB data acquisition system from the same brand. The charge amplifiers were replaced with charge-to-deltaTron™ amplifiers from B&K, which are known to be compatible with the impedance head from the same brand. The charge preamplifiers (or charge-to-deltaTron amplifiers) are used to amplify the force and acceleration signals from the impedance head and decrease their sensitivity to disturbances from cable capacitance. Picture 2 illustrates the setup used to measure MPI in the Swedish patients.

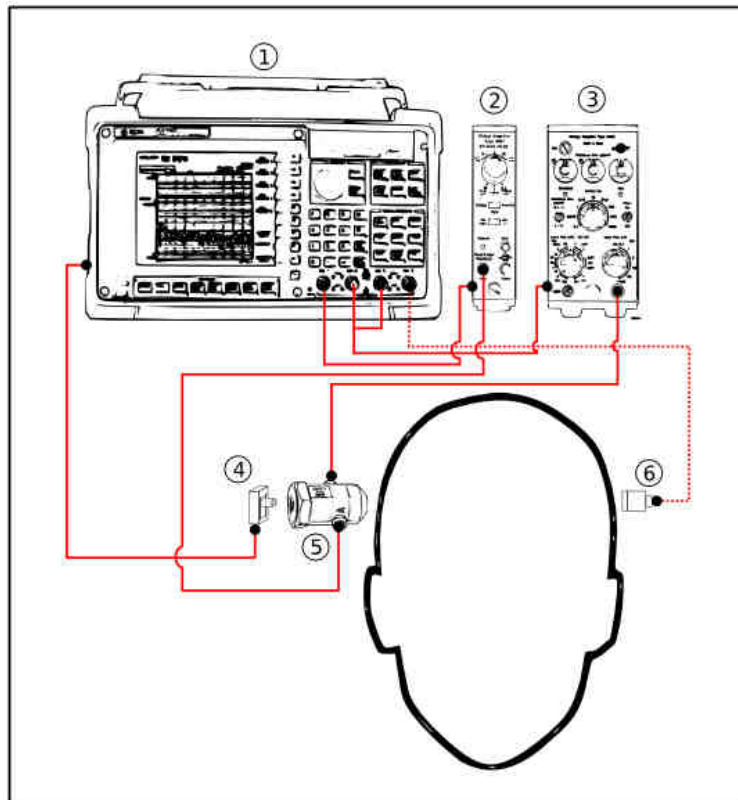For transfer accelerance function recording an extra accelerometer is needed. This setup can be seen in figure 3:

Figure 3 - Setup used for transfer accelerance function measurements in Sweden.
1- Agilent 35670A signal analyzer, 2- B&K 2635 charge amp, 3- B&K 2651 charge amp, 4- BEST transducer, 5- B&K 8001 impedance head, 6- IPC accelerometer.

Figure 4 shows the design differences between the Cochlear and Oticon snap couplings and the way each gets mechanically connected to the abutment from Cochlear.
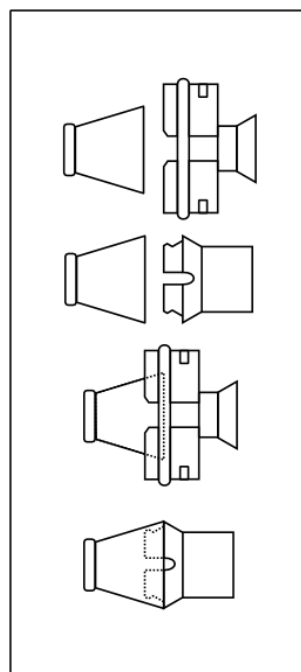

Figure 4 - Different coupling designs. Oticon Medical's coupling (1st and 3rd), Cochlear (2nd and 4th)

To be able to use the different couplings with the impedance head, adapters had to be built. Both the driving and the measuring side of the impedance head have 10-32 threaded female connectors. All couplings and abutments used had female M2 connectors on their free side. So every adapter built for this project consists on a 10-32 screw, with an M2 threaded hole through its longitudinal axis. This allowed the different couplings or abutments, to be connected to the 10-32 screw via an M2 screw.

In figure 5 a close-up image of how the different parts can be mechanically connected together is shown:
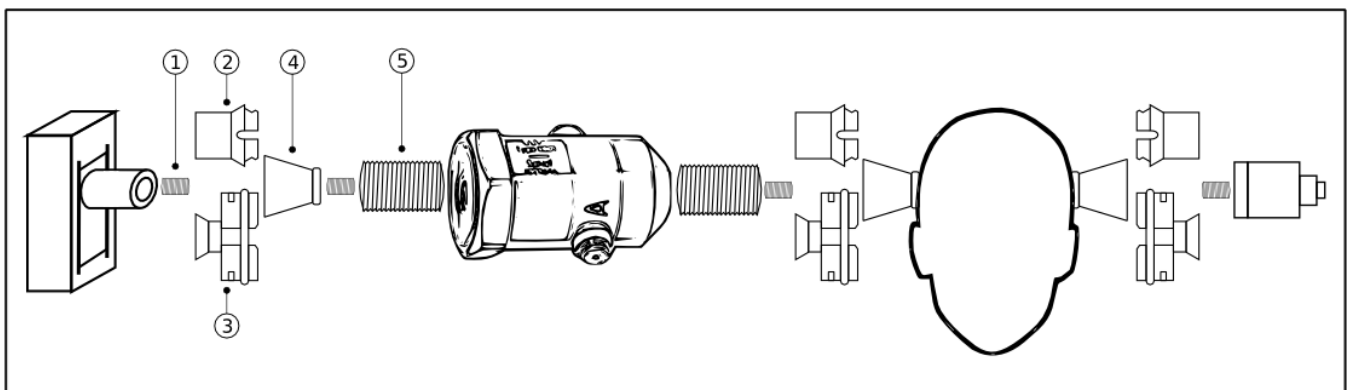

Figure 5 - Mechanical connections of different parts of the measurement setup.
1- M2 screw, 2- Cochlear coupling, 3- Oticon coupling, 4- Abutment, 5- 10-32 screw.

For every measurement, the couplings used between the transducer and the impedance head, and between the contralateral accelerometer and the abutment, was a Cochlear coupling. The reason to this was that by the time the adapters had to be built, there were many more cochlear couplings in stock in the lab.

Finally, figure 6 shows the setup used for the coupling comparison tests, and figure 7 shows the whole MPI measurement setup in an effort to give the reader a better understanding of the complexity of the system.
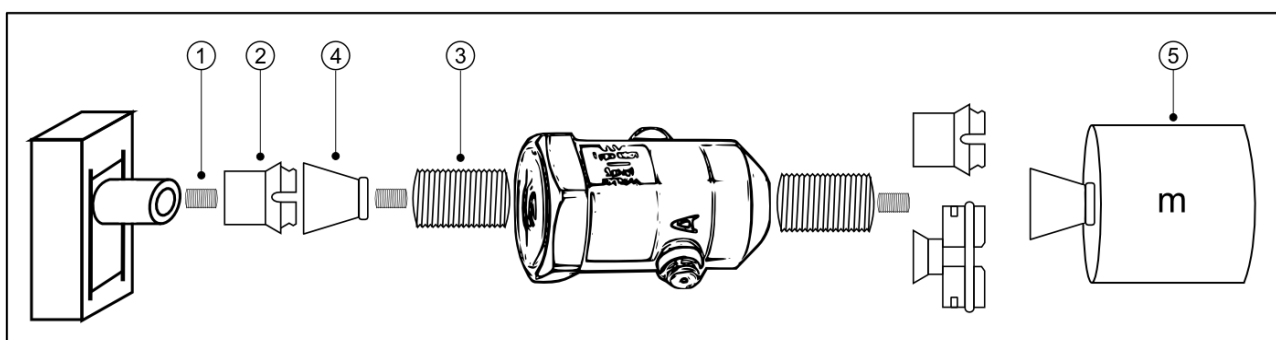

Figure 6 - Mechanical connections for MPI measurements on pure mass.
1- M2 screw, 2- Cochlear coupling, 3- 10-32 screw, 4- Abutment, 5- Pure mass
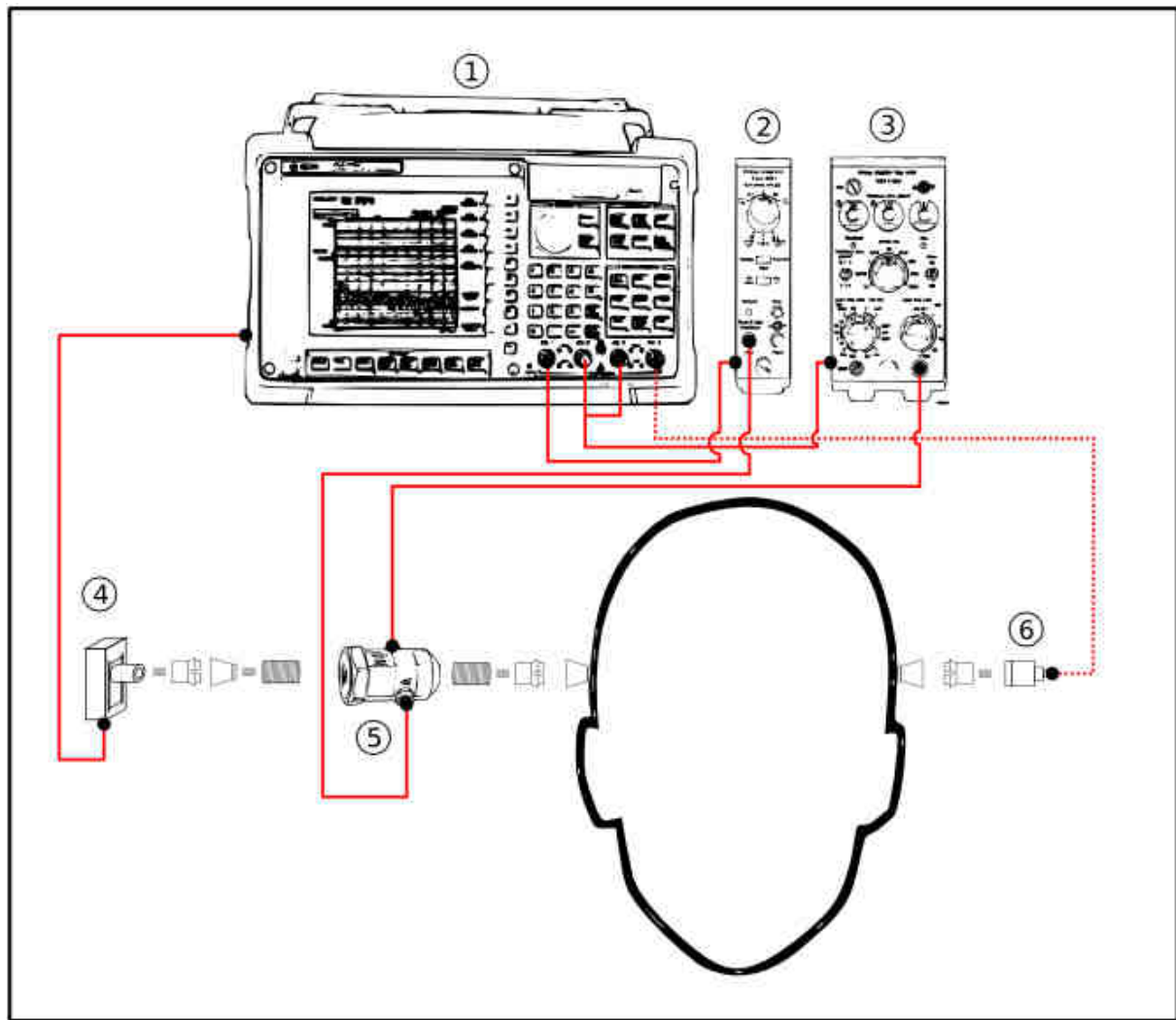
Figure 7 - MPI measurement setup.
1- Agilent 35670A signal analyzer, 2- B&K 2635 charge amp, 3- B&K 2651 charge amp, 4- BEST transducer, 5- B&K 8001 impedance head, 6- IPC accelerometer.

Measurement setup design

The measurement setup for recordings of impedance data from Swedish patients had already been used for an important number of studies in the past. Thus, it was provided to the author with most configurations already set to their correct value. The result of any measurement could be exported from the Agilent signal analyzer to a pc through a LabView program, and the result was a CSV-file with F/a magnitude or phase values and the frequencies at which these were recorded.

For the measurements in Canadian territory, instead, the equipment had recently been acquired by the iRSM for their Interfacial Biomechanics Laboratory, and had never been used before. A positive aspect of this fact was that modern equipment gives more versatile applications: it was highly possible to adjust the set up to the exact needs of this study. However, it proved to be a major task to achieve this.

The goal for the first phase of this project in Canada was to achieve a measurement setup equivalent to the one in Sweden, mostly because this latter one had been proven effective throughout the years. The signal analyzer from Agilent has a number of built-in functions that facilitated the measurement tasks in the early phases of this study. These corrections were applied by the analyzer in an automatic manner. Instead, for the new set-up being built, every single function was programmed and built from the ground up in LabView. A considerable number of weeks for programming and testing were needed to succeed in this assignment. The result was a LabView program (also called "virtual instrument") with the following as main features and abilities:

- Communicate with the data acquisition card for input and output at it's maximum sampling rate
- Excite the BEST transducer with a swept sine signal of customizable amplitude and frequency band.
- Record a customizable number of measurement points along the frequency band, with logarithmic or linear spacing between each point.
- Perform automatic calibrations between a pair of sensors with a known mass.
- Automatic sensitivity setup for known sensor types.
- Customize sensor sensitivities in a simple way, to be able to use different sensors.
- Record several simultaneous channels.
- Perform integration in the complex plane
- Display impedance (F/v) graph instead of the F/a being measured, at the same time as the swept sine measurement is being performed
- Display the signals through each channel as the measurements are being performed.
- Automatic numbering of patients
- Automatic data saving
- Switch between impedance- and transfer function measurements in a simple way.

Screenshots of the final LabView program can be seen in figures 34 to 37 in the appendix, while figures 38 to 40 in the appendix show examples of its source code.

This virtual instrument could output CSV files with patient number, measured side, and the following information for every measured frequency:

- Force channel data (RMS)
- Acceleration channel data (RMS)
- Phase component of impedance
- Magnitude component of impedance

Because of the output current limitations from the NI-cDAQ 9172, a battery operated current amplifier was also built for this study. It was capable of delivering 3 ampere continuously and peaks of up to 5 ampere, which allowed for direct driving of the BEST transducer from one of the daq's output channels.

Measurement procedure

In order to achieve measurements that were directly comparable with each other, being the case that the patients were measured in different countries and with different setups, a standard measurement procedure was developed.

The patients were received at the laboratory and they were given a simple explanation of what to expect to experience during the measurement. They received an informative document about the purpose of the study. They also received a questionnaire that they had to fill and sign, allowing us to use their data on the study.

They were asked to sit in a normal upright position on a chair without head rest. After the whole setup was connected and ready, the measurement was started and it lasted for approximately 40 seconds for each measured side.

To be able to perform the measurements in this position it was first tested that the load and momentum of the transducer + impedance head system, as well as their cables' weight, did not affect the impedance measurement results. This was achieved by performing impedance measurements with a dry skull and the same setup, but rotating the dry skull and thus changing the angle in which the impedance head and transducer perform the excitation. No major differences were found when changing this angle, so it was concluded that the patients would be allowed to sit in an upright position.

Another important step before the measurements can be done is to establish what voltage to feed to the transducer in order to induce a vibration that corresponds to a certain hearing sensation. This is of extreme importance, firstly because it would be unacceptable to over-drive the patients' skull causing them discomfort. Also, because if this level is too low, it would increase the chances of the measured values being affected by measurement noise.

In "*Force threshold for hearing by direct bone conduction*" (Carlsson, 1995) it is stated that 0 dBHL correspond to an excitation of 45 dB with reference level 1 µN at a frequency of 1 kHz. This corresponds to applying a force of 200 µN at a frequency of 1 kHz. It was decided that an acceptable level of excitation without risking patient discomfort would be of 40 to 60 dBHL. 40 dBHL corresponds to an excitation force one hundred times higher that our ground level of 0 dBHL: 0.02N at a frequency of 1 kHz.

To be able to know which feeding voltage would lead the transducer to apply the desired force at the desired frequency, a series of measurements was performed on a pure mass while varying the voltage and observing the force output being measured by the impedance head. This way it was possible to establish that a feeding voltage of 56 mV RMS would cause the BEST transducer to apply the force that corresponds to 40 dBHL.

The measurements were all performed in 401 points logarithmically spaced along the frequency band 100 Hz to 10 kHz in what is called a swept-sine measurement. The equivalence of both measurement setups was also studied; the outcome of this comparison is presented in the Results section.

Calibration

Connected to the implant, there are several masses that need to be taken into consideration for calibration purposes: a mass before the force gauge, *m1* (often given in the impedance head's manual), and possibly an adapter to be able to mechanically connect everything together, with mass *m2*.

To calculate a calibration constant *k_c*, a known mass *m3* that can be mechanically connected to the impedance head needs to be used:

$$M_{tot} = \frac{F}{a} \cdot k_c \qquad (2)$$

m_tot = m3 + m2 + m1 is already known. The force and acceleration quotient can be obtained by running a regular measurement with the setup mentioned before. This quotient should theoretically be shown in the magnitude graph as a constant value, namely, the total mass. In practice, depending on the used impedance head's characteristics and performance in different frequencies, it will show a slight ripple. So in means of data, a vector of values instead of a constant is derived from the measurement. For this calibration purposes, it has been assumed that the error shown as ripple will not behave in the same manner for each measurement. So instead of measuring this quotient on a known mass before each measurement, which would be very time consuming, the quotient value at 1000 Hz was used as an indicative measure of the whole frequency range. This way, a single constant is used instead of the whole vector containing Q = (F / a). Finally the calibration constant can be derived from:

$$k_c = \frac{M_{tot}}{\frac{F}{a}} = \frac{(m_1 + m_2 + m_3)}{Q} \qquad (3)$$

Mass compensation

The measuring side of the impedance head records information about everything that is mechanically connected to it. That means that even the adapter and the snap coupling, as well as the impedance head own mass before force gauge, are included in the patients impedance measurements unless a compensation for these masses is made to avoid this.

With k_c known from (3), adjusting the measured quotient Q can be done in the following way:

$$Q_{adjusted} = Q_{measured} \cdot k_c - (m1 + \ldots + mn) \qquad (4)$$

where m1...mn are all the masses that should not be included in the measurement, i.e. the mass of those other than the patient's head, implant and abutment.

For the measurements performed in Canada, integration was automatically made by the LabView interface, so the resulting file contained impedance data instead of the quotient F/a. To be able to perform a correct mass compensation, the F/v data was processed in the following way:
   1. Reconstruction of complex number from phase and magnitude data.

2. Derivation of complex F/v data
3. Calibration of derivated complex F/a data.
4. Mass compensation of complex F/a data.
5. Integration of complex F/a data into F/v.
6. Separation of complex F/v data into magnitude and phase vectors.

Impedance calculation

Once the quotient Q = F / a has been measured, the impedance curve can be calculated. From (1) integration is needed in order to get to the desired impedance, which in practical terms, and because the measured ratio is in the frequency plane, can be achieved by multiplying by the imaginary constant j and the frequency omega:

$$Z = Q \cdot \frac{1}{j \cdot \omega} = \frac{F}{a \cdot j \cdot \omega} = \frac{F}{v} \qquad (5)$$

Data processing

The high number of measurements performed during different phases of this study resulted in a considerable amount of data. Different standards were developed to facilitate the programming of functions for information extraction from the files containing the patient data.

A matlab library called MPI_lib.m was written. It contains over 20 functions that take advantage of the developed standards and facilitate several different tasks. Among others we can find:

- handling data parsing from CSV and Excel files
- formatting of data
- performing integration and integration to the data in the complex plane
- converting the data into different domains
- applying suitable calibration constant depending on the equipment used to record the data
- showing magnitude and phase graphs with customized format
- calculating confidence intervals around a certain mean
- perform adequate mass compensation
- exporting resulting figures to PDF, JPEG, or FIG files

All the functions contained in the library were capable of being called and used from every other program developed for this study through a function handle.

A number of other programs in the same programming language were written to aid the author in some repetitive programming tasks. It is of extreme importance that a certain patient's data isn't mixed with that of another patient, or with data recorded from other sources or channels. Any mistake in this could result in wrong or meaningless results. These "helper" programs had the capability of writing Matlab code for the main data processing program in a safe way, avoiding misspelling and considerably speeding the whole process up.

The source code for the different programs and scripts is not included in the appendix of this report as it was planned because of its size of over 2000 lines of code.

Modeling

Another goal for this research project was to try to find a mathematical model that explains the measured mean for the mechanical point impedance.

The first intended approach was to try to optimize the model proposed by previous studies. The model consisted in an electric circuit containing a number of different inductors, capacitors and resistors, and this first approach aimed at the optimization of their values. The model was built in simulink, with the SimPowerSystems™ toolbox and analyzed with an impedance measurement block. It was then improved by changing the values of every component manually, while observing the changes in circuit's impedance behavior. After failing to automate this process, this approach was abandoned for being too time consuming.

Different modeling techniques were tested after the previous one, amongst others: linear parametric modeling, process modeling, spectral modeling and correlation modeling. The tool used now was the System Identification Toolbox in Matlab. The frequency function data used was the smoothed version of the mean MPI magnitude and phase from all 45 patients. The reason to use the smoothed data is that it doesn't have as many noise spikes in the low frequency region as the non-smoothed version. It is also easier to model, which makes the optimization task faster.

One model was built with the predefined configuration of each technique. These initial models were optimized a number of times and their performance was observed throughout this process.

Observing the mean measured impedance magnitude and phase it is noticeable how similar its behavior is to that of a second order model. The models with best initial performance were chosen for further optimization and for this case all of the models chosen happened to be second order models created with the process modeling tool.

These chosen models were optimized further until a plateau was reached, at which new iterations of the optimization process did not result in additional model improvement.

Figures 8 and 9 show screenshots of two of the tools provided by the System Identification Toolbox for model fit analysis.
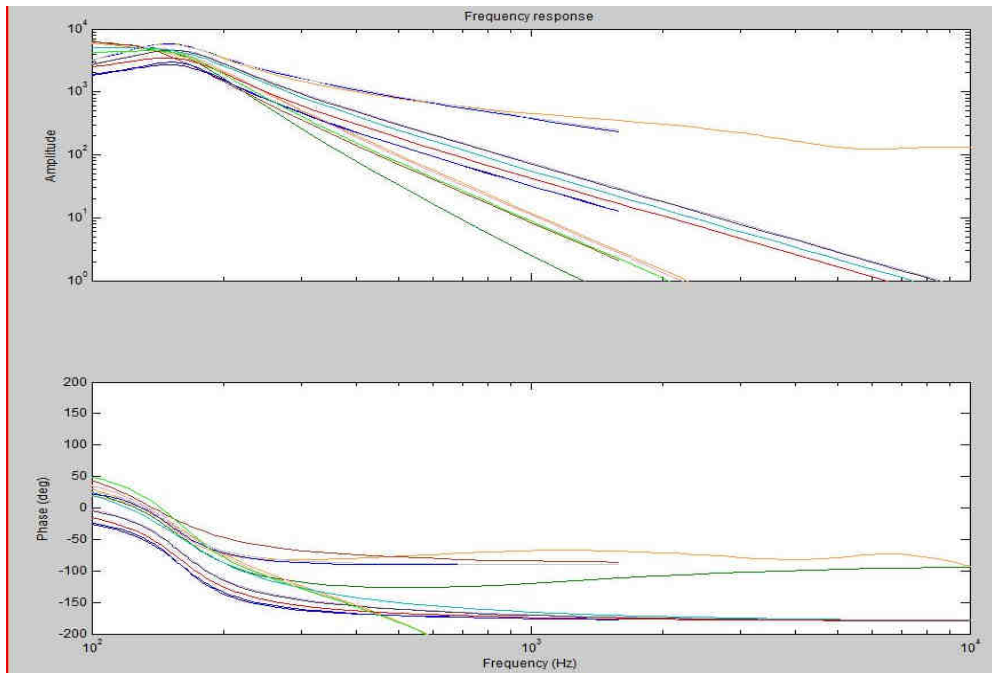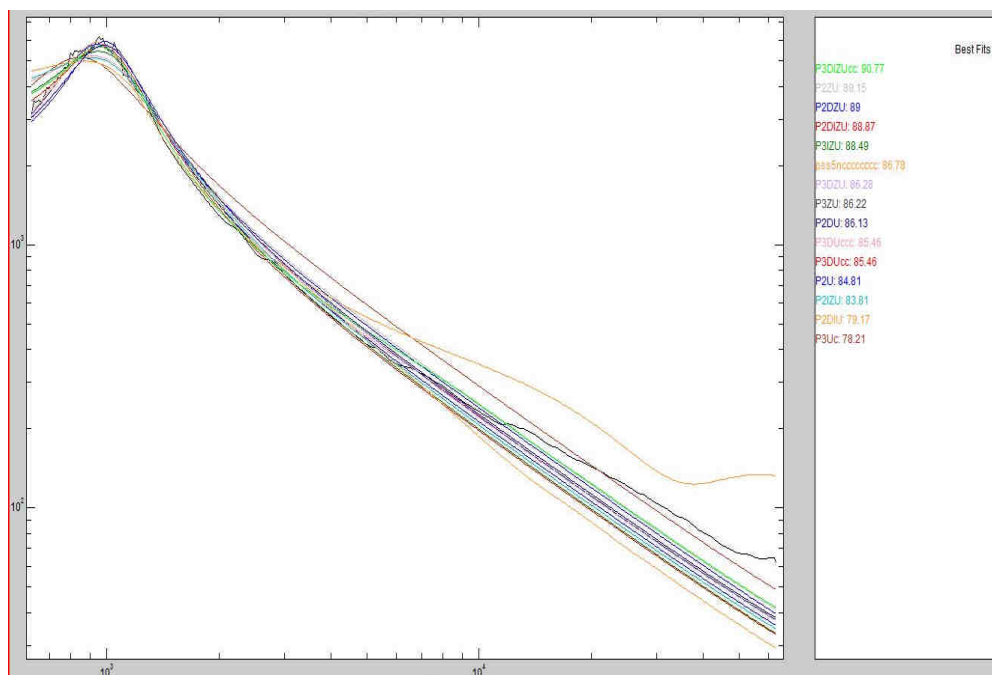
Figure 8 – Frequency response tool window

Figure 9 – Model output tool window

The plots in the Model output window show the simulated outputs of the models selected in the system identification session. The models are fed with inputs from the chosen Validation Data set. The Validation Data set is plotted in black in the same window, allowing for visual comparison with the output of different models.

When using Frequency Function data, as in this case, the Model Output window shows the amplitude curves of the data's and the different model's frequency responses. The percentage of the output variations that is reproduced by the model (called "fit") is displayed at the side of the plot: a higher percentage number means a better model.

20

The precise definition of the represented fit is:

$$FIT = \frac{1 - NORM(Y - Y_{sim})}{NORM(Y - MEAN(Y))} \cdot 100 \qquad (6)$$

where Y is the measured impedance data and Y_{sim} is the simulated model output.

The Frequency response window adds phase information to the analysis of the different models, but lacks of information about model fit. Both tools were used together for this project.

Statistical significance

In an effort to try to understand the impact of patient characteristics on their skull's impedance, the patients were divided into groups. The groups were built based on a common patient parameter or attribute, or the absence of it, and the mean impedance of each group was calculated and plotted. The intention was to study whether the graphs of the different mechanical impedances showed a difference in behavior that could be interpreted as proceeding mainly from that specific parameter.

Statistical significance is a mathematical tool used to determine whether the outcome of an experiment is likely to be due to chance, if it's the result of a relationship between specific factors instead. A graphical way of studying this is to plot the XX% confidence intervals of each mean and check whether they overlap or not. If there is a difference in the means, and their confidence intervals do not overlap, you can be certain with probability P<(100-XX)/100 that the difference is of statistical significance. The higher the confidence level wanted, the bigger the size of the confidence intervals, thus, the harder it is to find a statistically significant difference.

The size of the confidence intervals is also dependant on the sample size. Because the main objective of this research project was to find a general mean and not to study these differences, in many cases the different groups are populated with a small number of patients. This enlarges the size of the confidence intervals significantly.

For the groups whose graph shows a certain tendency, additional graphs were created where the depicted means are shown together with their 80% confidence intervals.

5.   Results

In this section, a series of graphs showing measurement results are presented. The frequency axis is logarithmic, and the data covers the frequency band 100 Hz to 10 kHz. The y-axis for the magnitude plots is also logarithmic, whereas the y-axis of the phase graphs is linear.

Mechanical point impedance measurements

The magnitude and phase of the measured skull impedance on all 45 patients are presented in figure 10. Figure 11 shows the mean measured value for all patients in magnitude and phase, as well as the 80%, 90% and 95% confidence intervals at each frequency point. Patients 19 and 22 were not included in the results due to administrative problems.

The magnitude plots presented in this section show an antiresonance (also called parallel resonance) in the lower end of the frequency range. Most often, this happens between 100 Hz and 250Hz. Some patients' skull showed this antiresonance even before 100Hz, which was observed by running a new impedance measurement on them (not included in this work) in the frequency range 50 Hz to 150Hz.

In frequencies lower than that of the antiresonance, the impedance shows a positive slope in the magnitude, and a positive phase angle. This corresponds to a mass-controlled impedance behavior or, in the electronic domain, to an inductor-governed behavior. For frequencies above that of the first antiresonance, the impedance magnitude shows a negative slope and a negative phase angle. This corresponds to a dominant stiffness behavior in the mechanical plane; or to an impedance mainly ruled by a capacitor in the electrical world. Above approximately 175 Hz the phase takes values between -70° and -90°. For the mean of all p atients in this study, the antiresonance occurs at 147 Hz. At this frequency, the mean phase should cross the 0° line but it doesn't. The explanation is that the system also has some resistive components.

Some of the images were smoothed using a moving average method with span 5, mostly to delete the spikes generated by noise at low frequencies. These images are marked with "(smoothed)" in their caption. For example, figure 14 and 15 are smoothed versions of the mean impedance with the 80%, 90% and 95% confidence intervals at each frequency point.
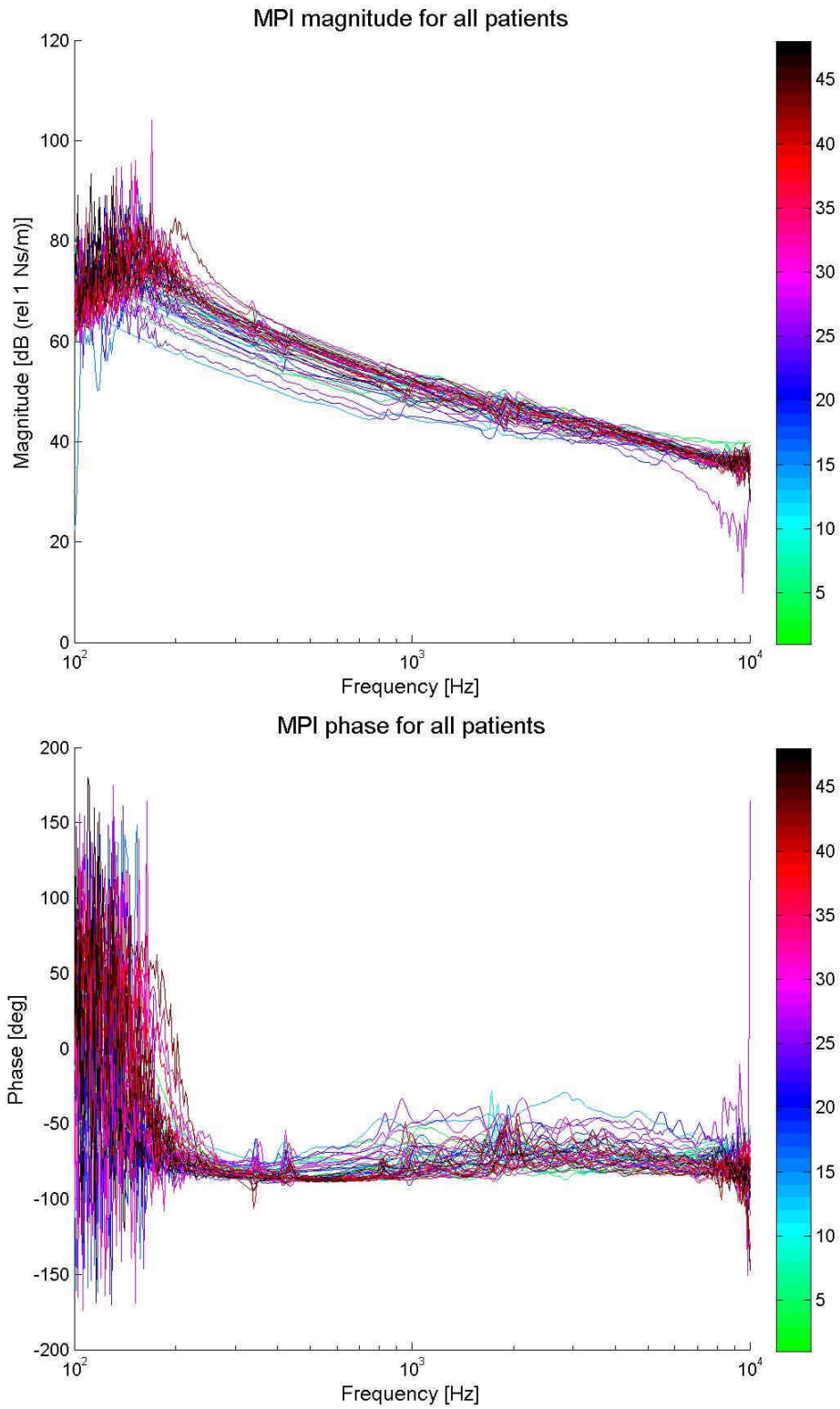
Figure 10 – MPI magnitude and phase for the 45 measured patients
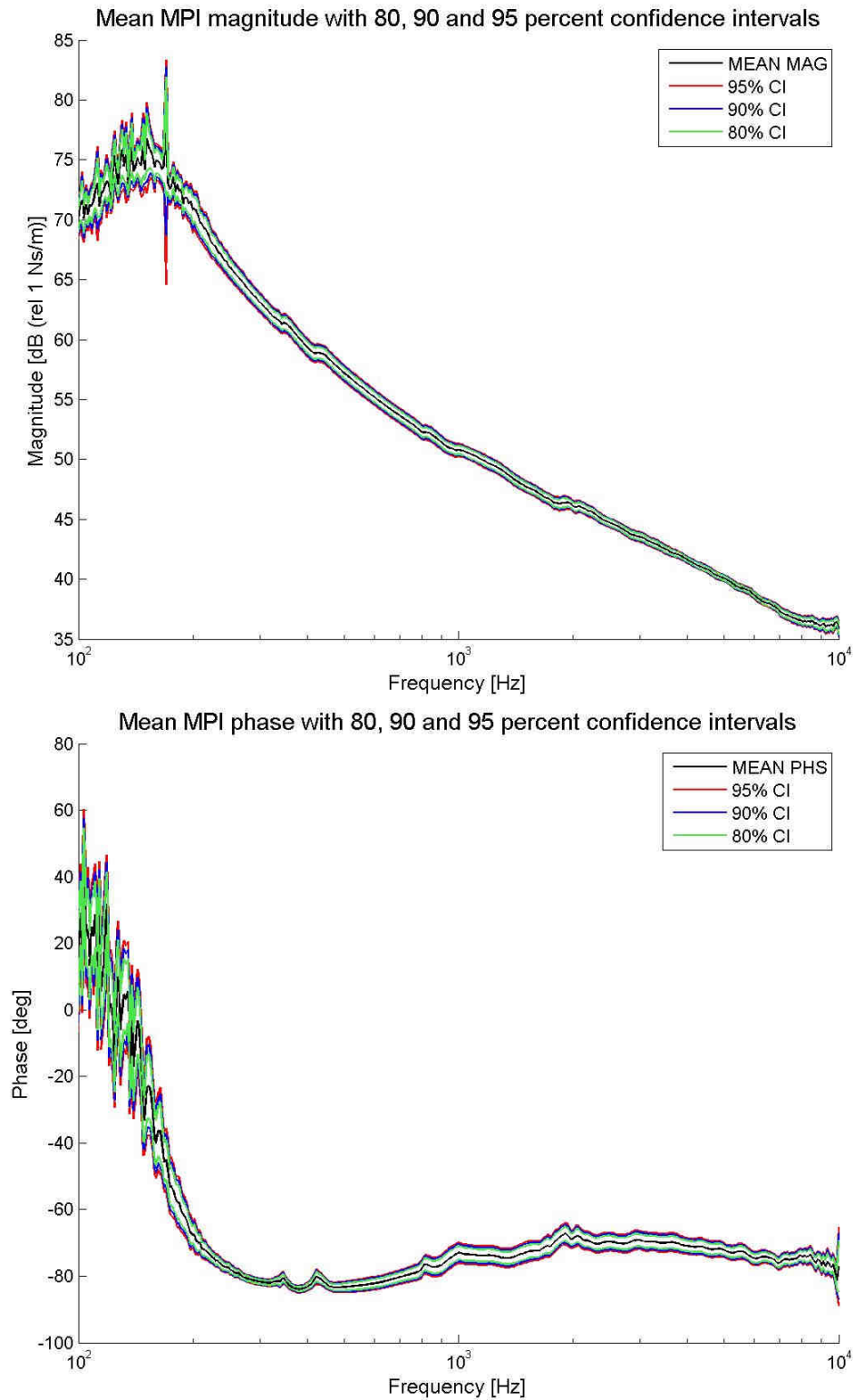
Figure 11 - Mean value of the MPI magnitude and phase at each measured frequency and the 80%, 90% and 95% confidence intervals
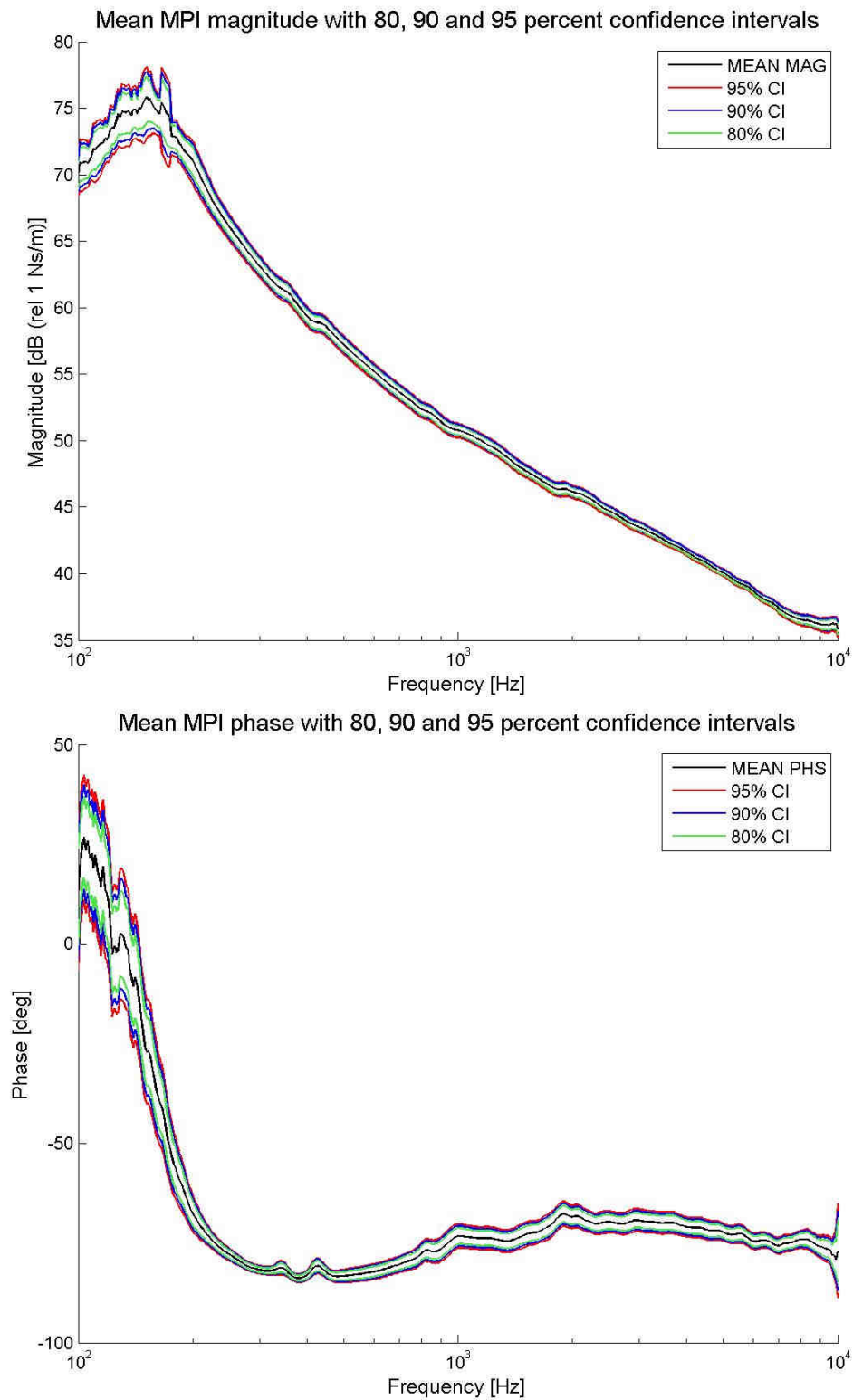
Figure 12 - A five-point moving average smoothing of figure 11. (smoothed)

In the following pages, the mechanical impedance for different patient groups is shown. The groups were built based on a common patient parameter or attribute, or the absence of it. The intention was to study whether the graphs of the different mechanical impedances showed a difference in behavior that could be interpreted as proceeding mainly from that specific parameter, and also how likely it is that a certain result is due to chance.

Figure 13 depicts the mean mechanical point impedance magnitude and phase for patients with no known diseases or abnormalities in skull anatomy.

Figures 14 and 15 show the mean MPI magnitude and phase for male vs. female patients.

In figure 16, the patients have been divided into three age groups and their means are plotted. Each group is defined by the patients' year of birth, covering approximately 20 years each: 1931 to 1949 (first group), 1950 to 1969 (second group) and 1970 to 1993 (third group).

The measured patients were born between 1931 and 1993. Their age spans then from 18 to 80 years old, covering an age-range of 62 years. Patients can then be classified into two groups, with an age limit of 18+62/2 = 49 years. Picture 17 shows the mean MPI magnitude and phase for patients older and younger than 49 years old.

Patients were divided into two additional groups with regards to age. The intention was to try to study further the tendencies seen at the graphs for previous age groups. The mechanical impedance for the older half of the patient pool was therefore plotted vs. that of the younger half of the patient pool in figures 19 and 20.
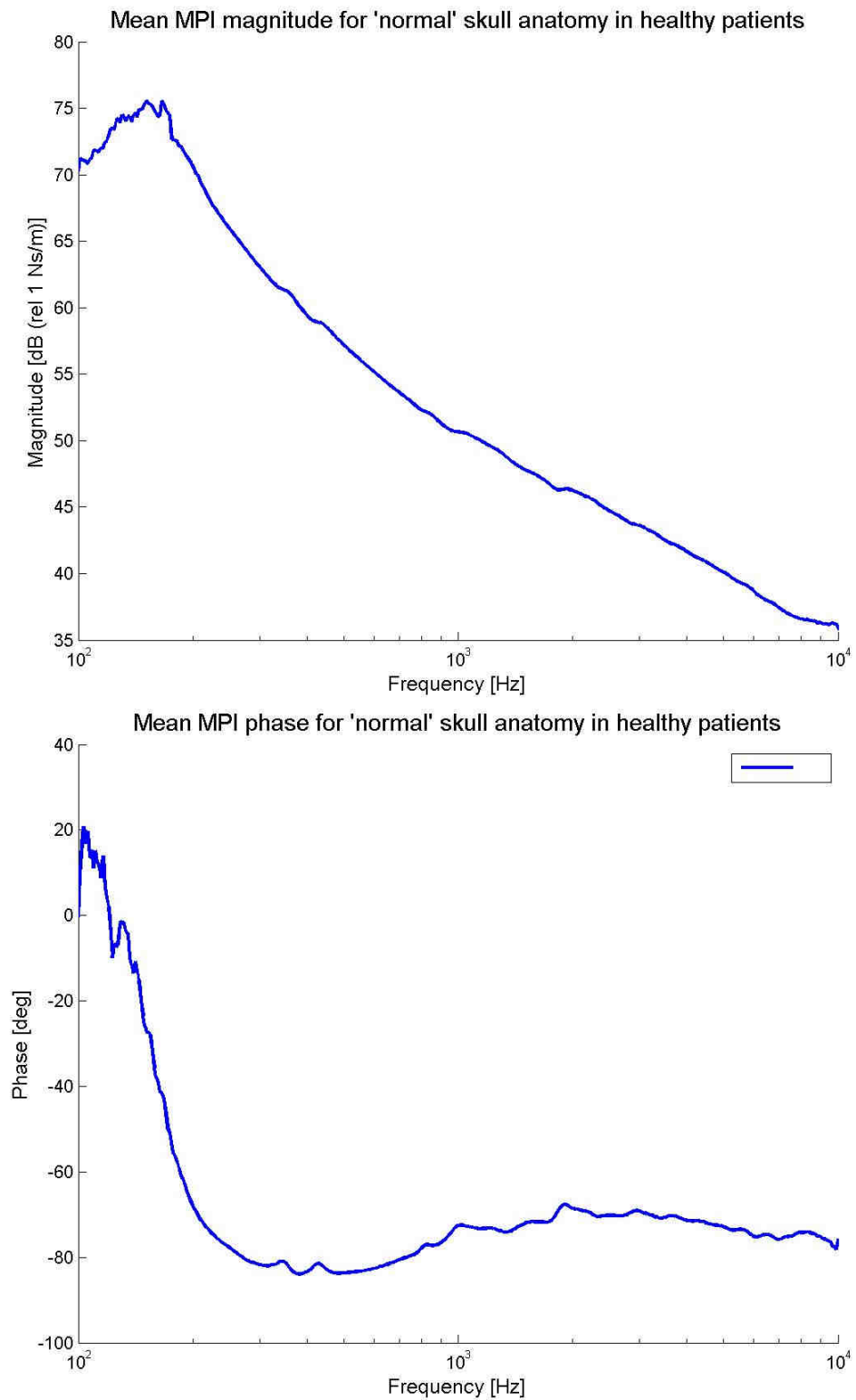
Figure 13 - Mean MPI magnitude and phase of patients with no known abnormalities or pathologies. (smoothed)
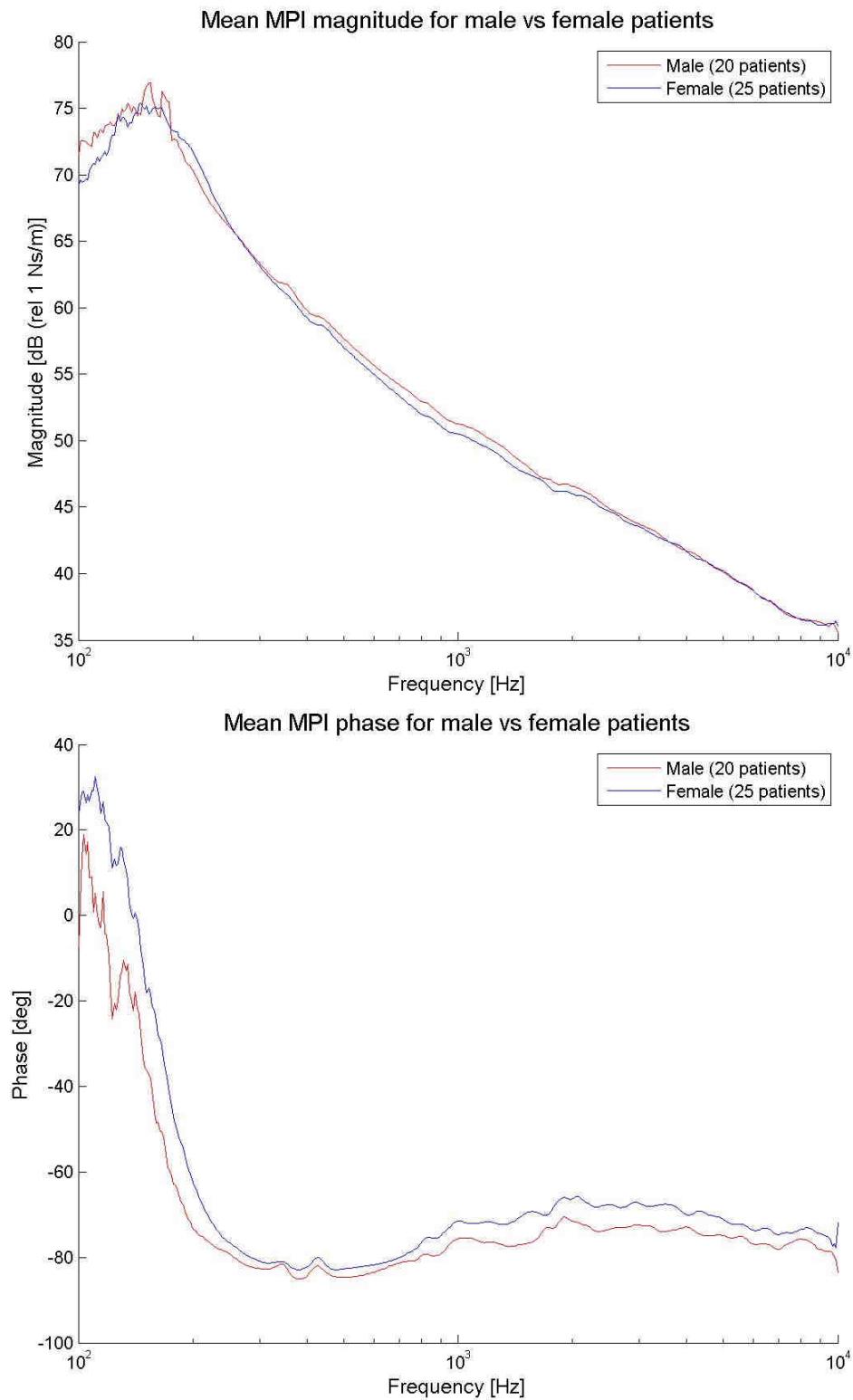
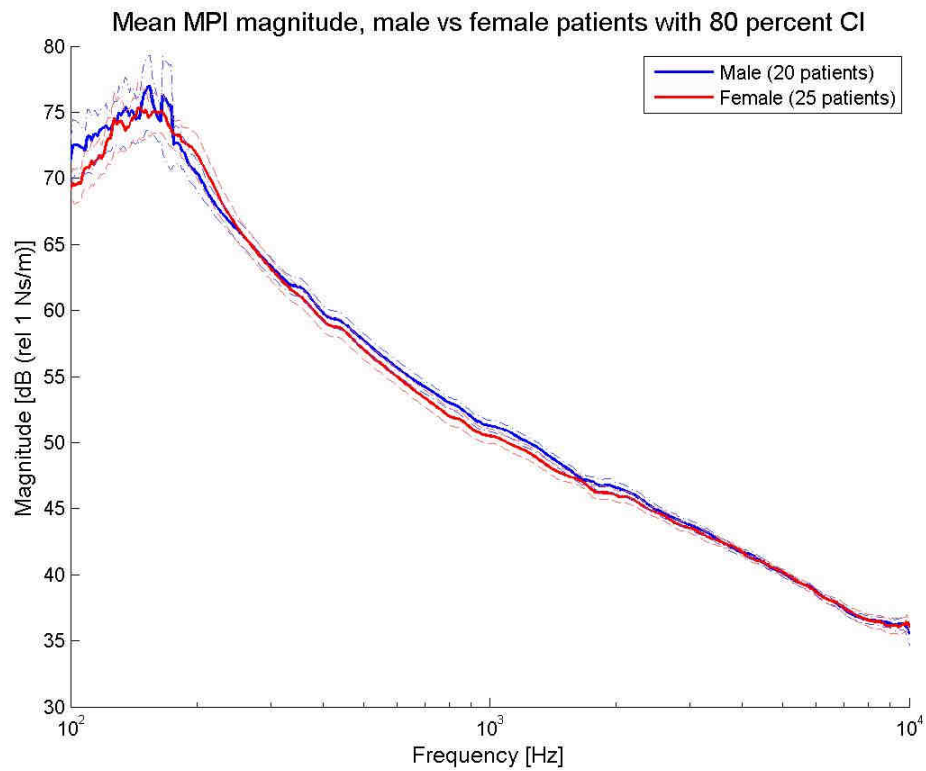**Figure 14 – mean MPI magnitude and phase for male vs female patients. (smoothed)**

Figure 15 – Mean MPI magnitude for male and female patients with their 80% confidence intervals (dotted lines). (smoothed)
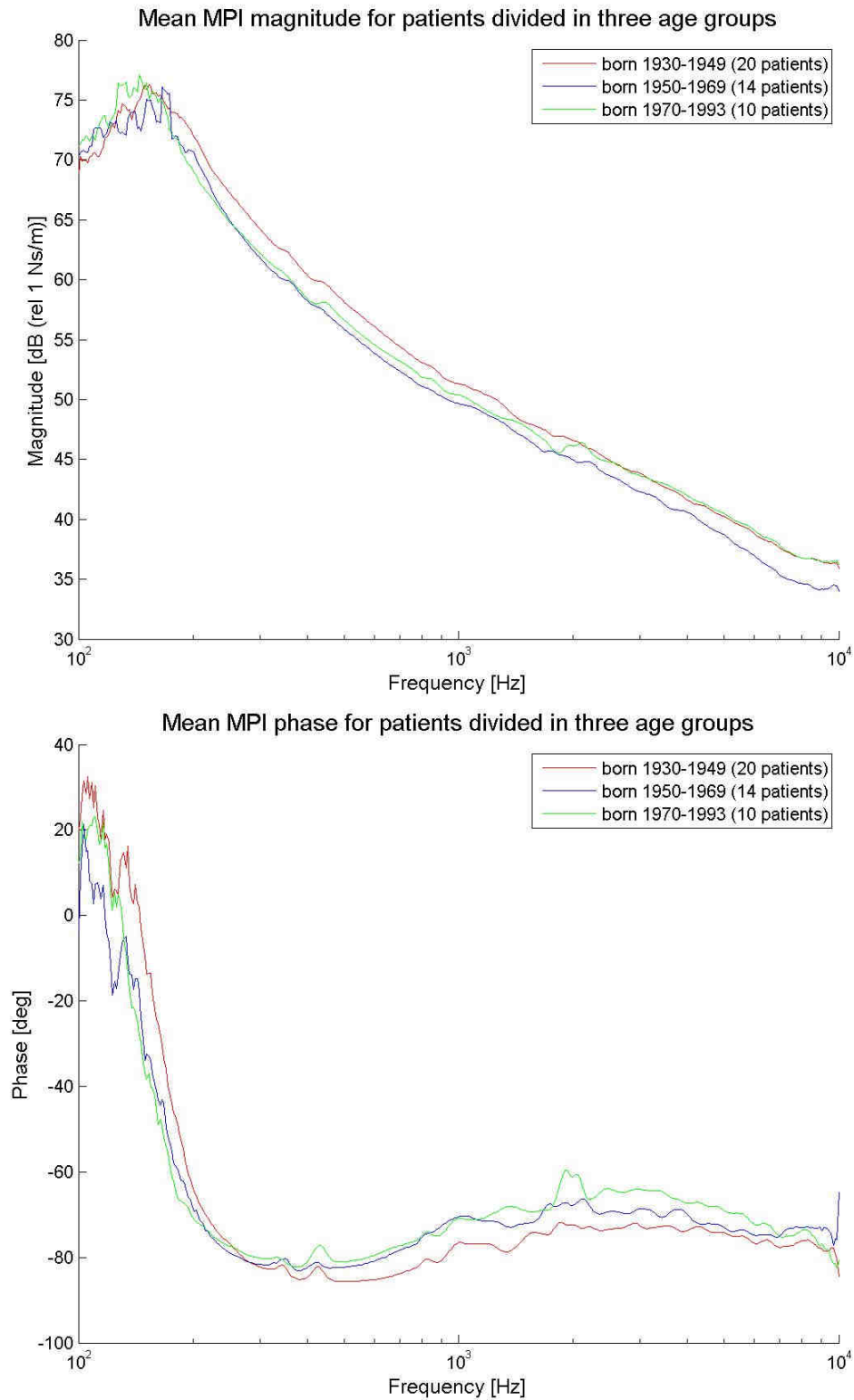
Figure 16 – Mean MPI magnitude and phase of patients of different age groups. Each group corresponds to approximately 20 years. (smoothed)
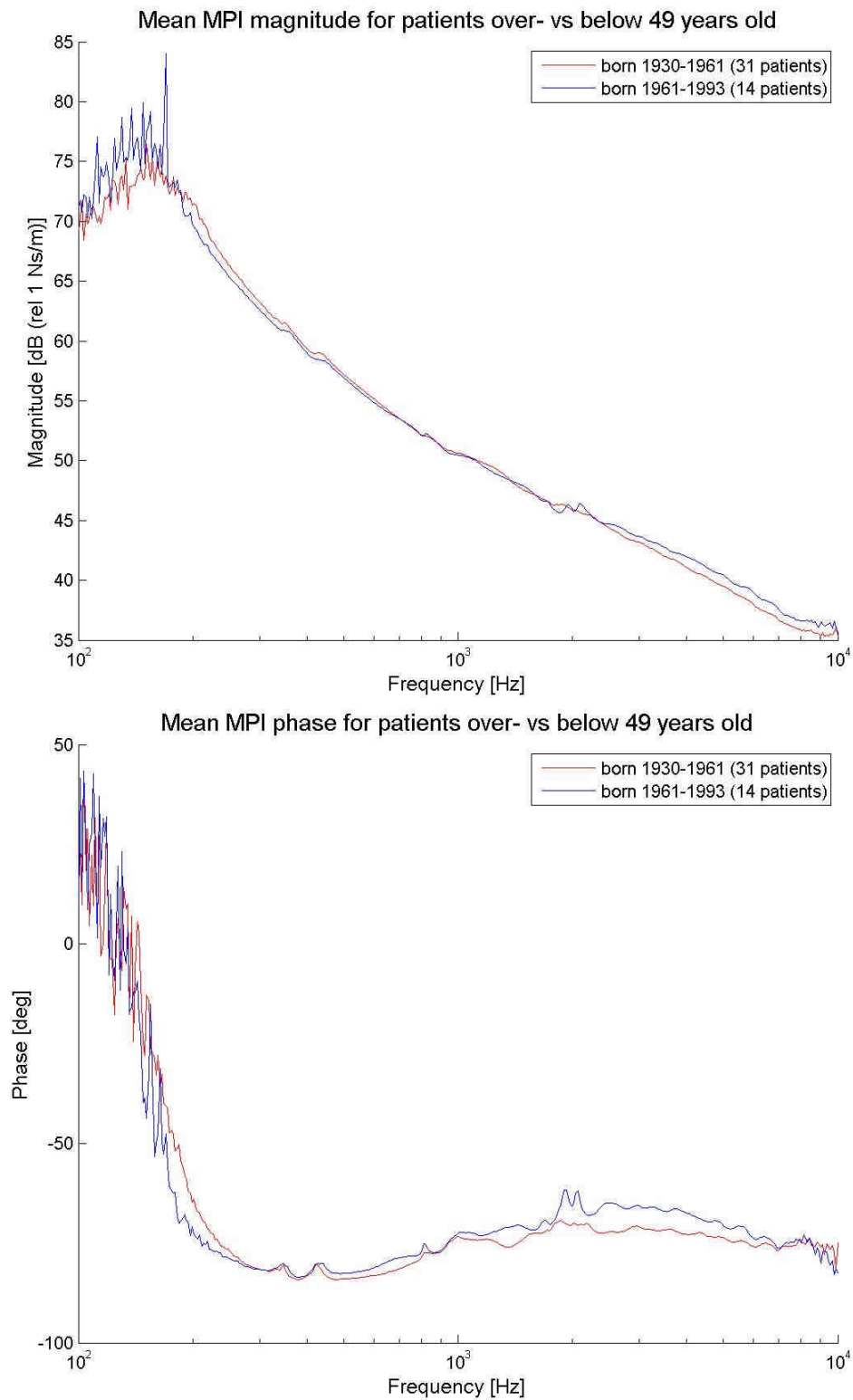
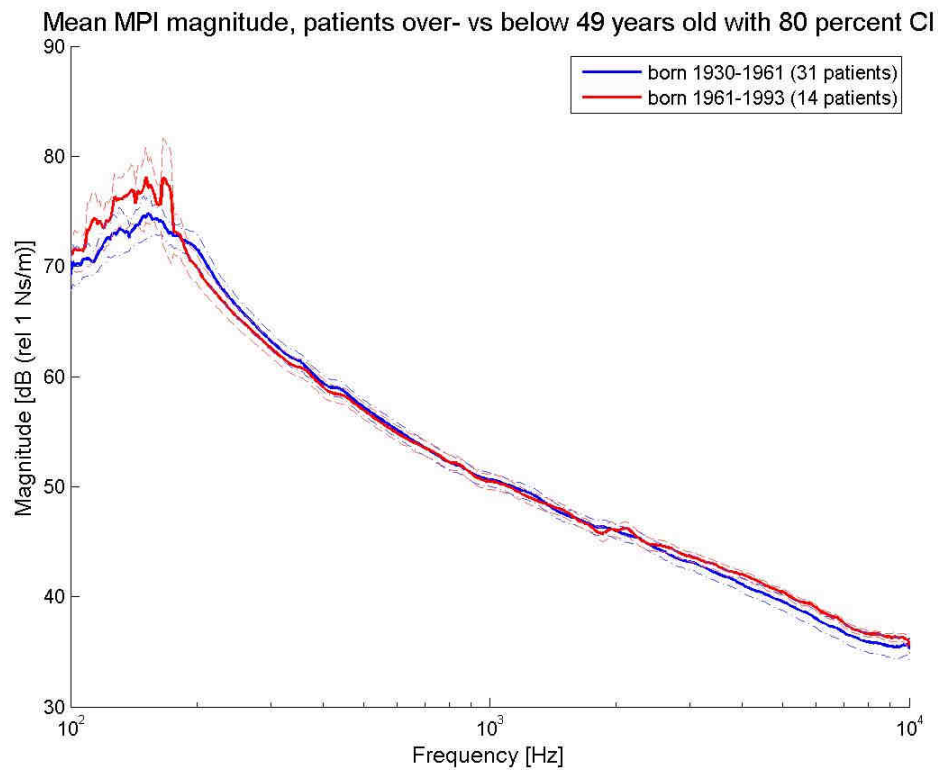**Figure 17 – Mean MPI magnitude and phase of patients above and below the median age of 49 years. (smoothed)**

Figure 18 - Mean MPI magnitude of patients above and below the median age of 49 years with their 80% confidence intervals (dotted lines). (smoothed)
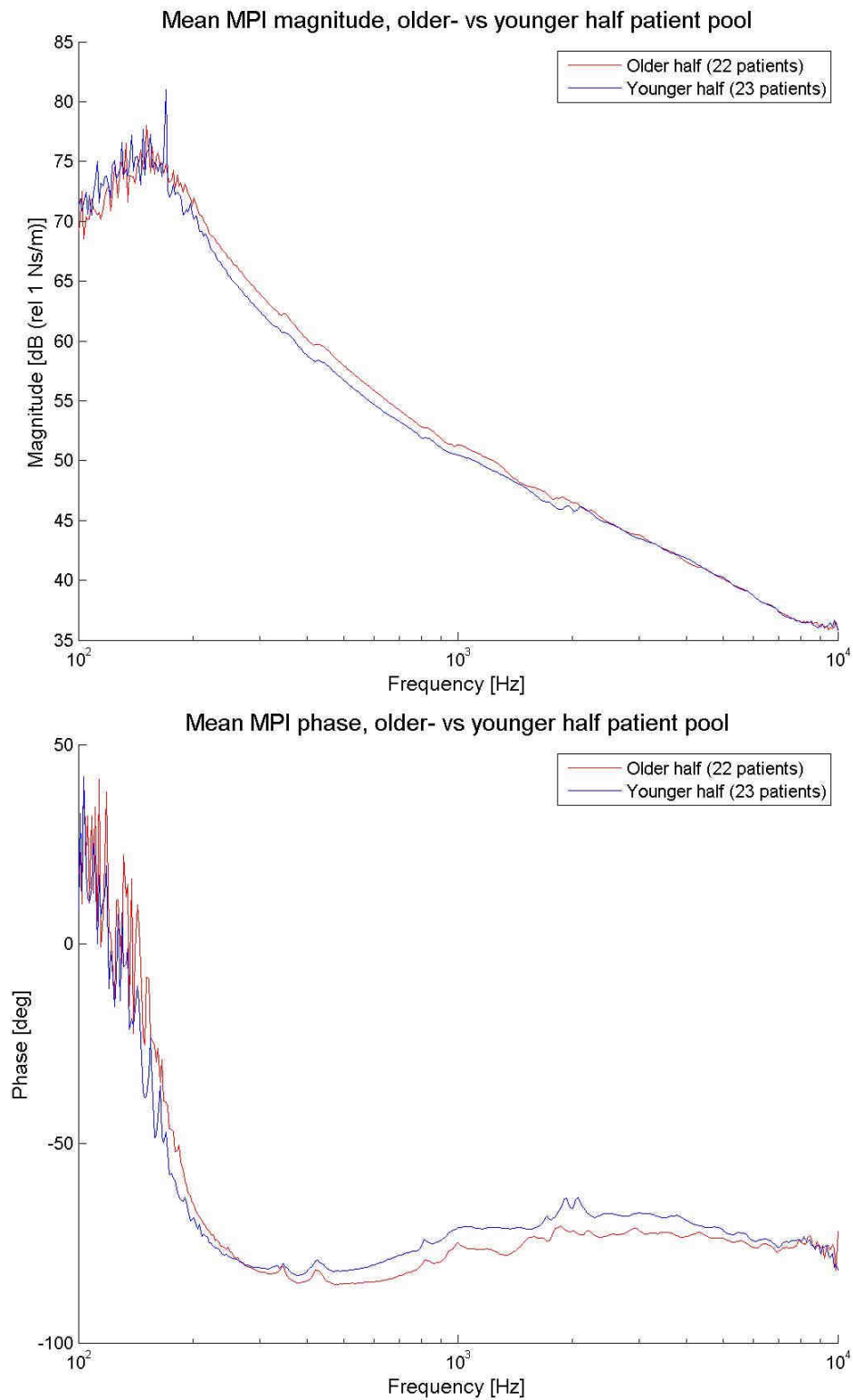
Figure 19 - Mean MPI magnitude and phase of the older half of the total patient pool vs those of the younger half. (smoothed)
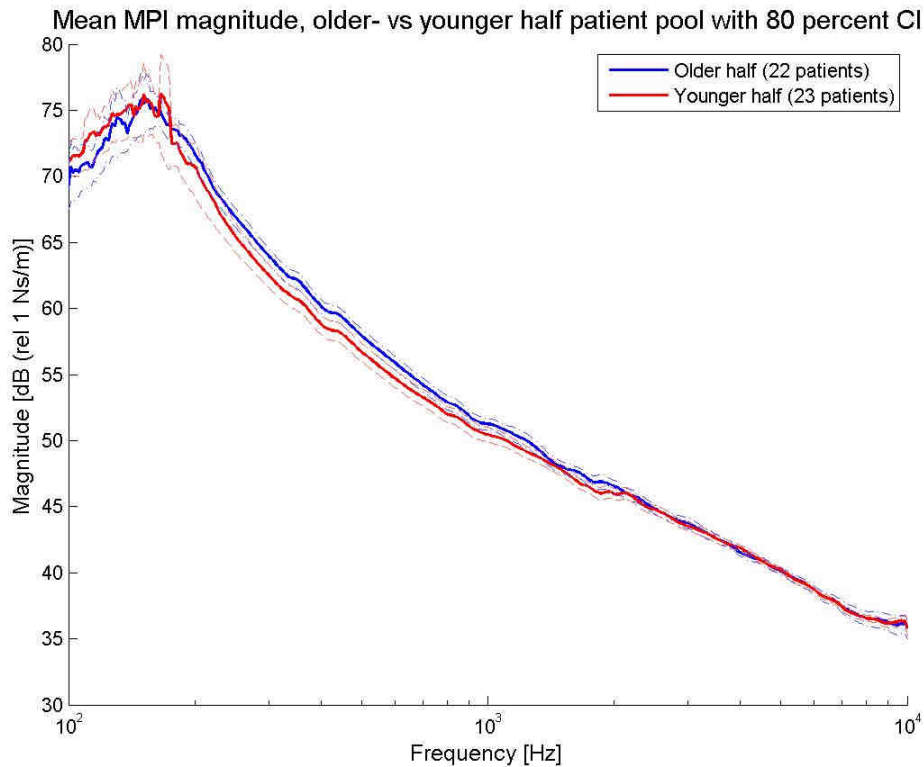
Figure 20 - Mean MPI magnitude of the older half of the total patient pool vs the younger half, with their 80% confidence intervals (dotted lines). (smoothed)

Figure 21 shows the mechanical point impedance magnitude and phase from patients with no known abnormalities in skull anatomy vs patients diagnosed with a specific syndrome known to affect craniofacial anatomy.

Pictures 22 and 23 show the mean MPI magnitude and phase of patients that have undergone ear surgeries suspected to affect the skull bone in the measured side vs. those patients that haven't.
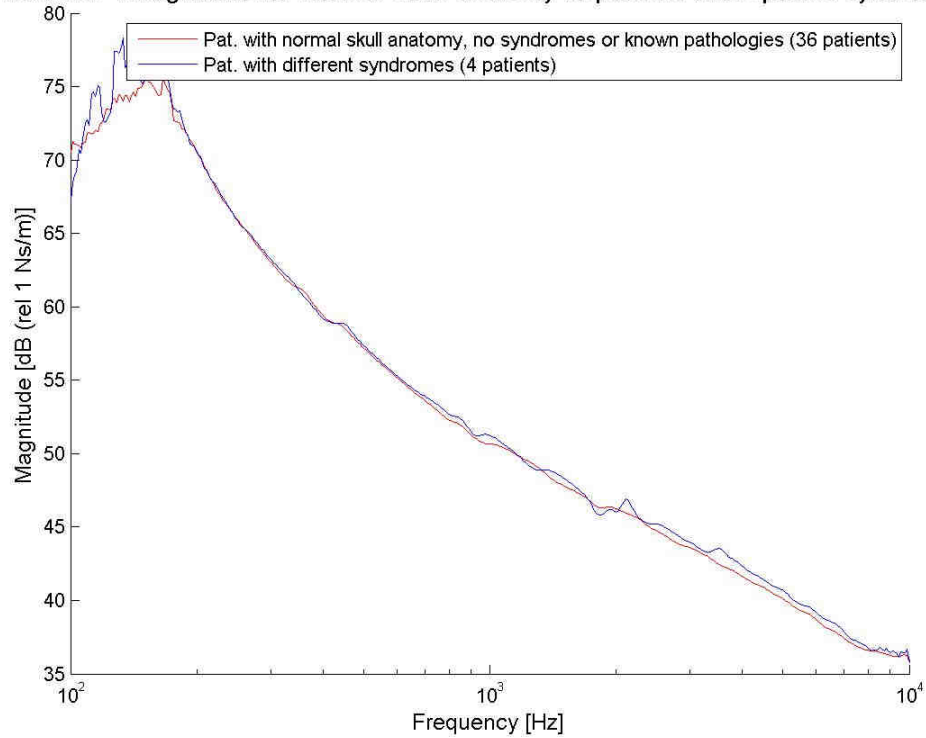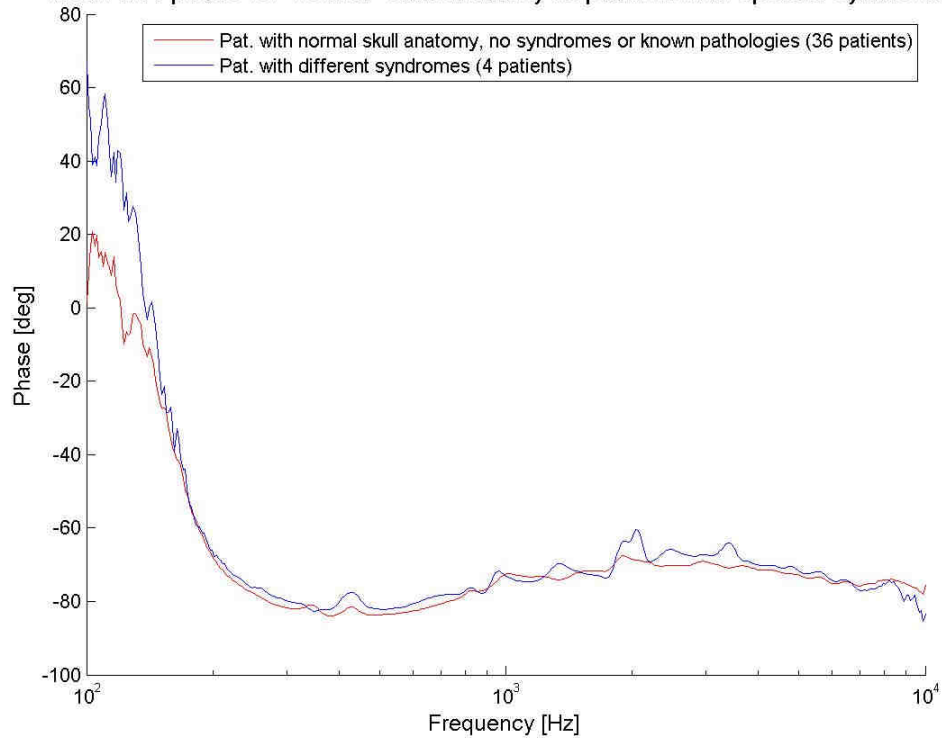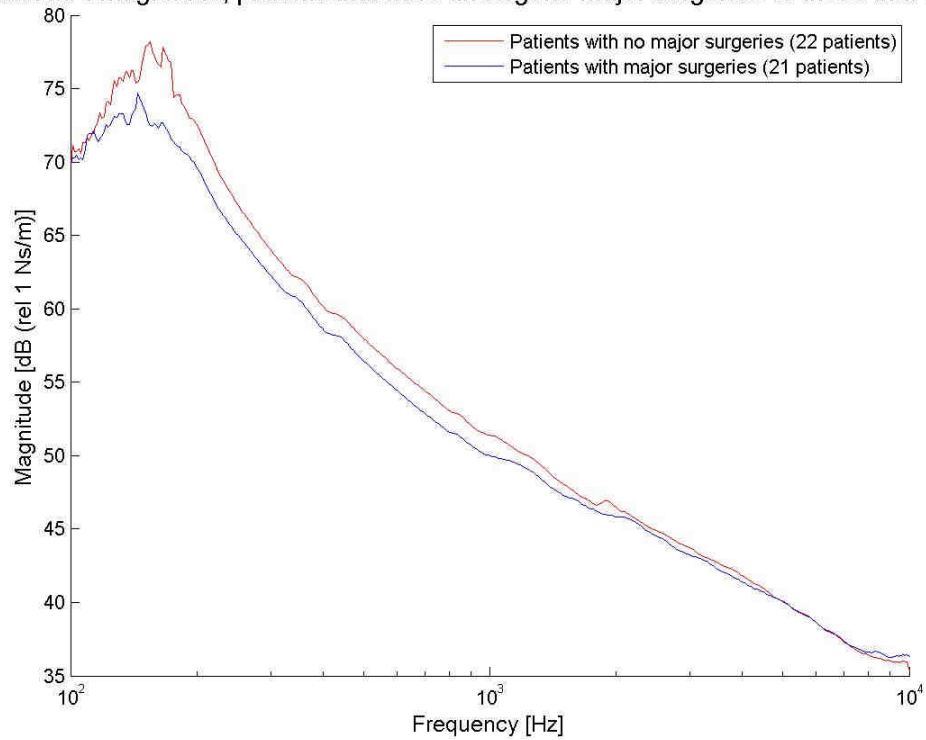
Figure 21 - Mean MPI magnitude and phase of patients with no known abnormalities in craniofacial anatomy vs that of patients with specific syndromes known to affect craniofacial anatomy. (smoothed)

Figure 22 - Mean MPI magnitude and phase of patients that have undergone major ear surgeries vs those of patients that did not. (smoothed)

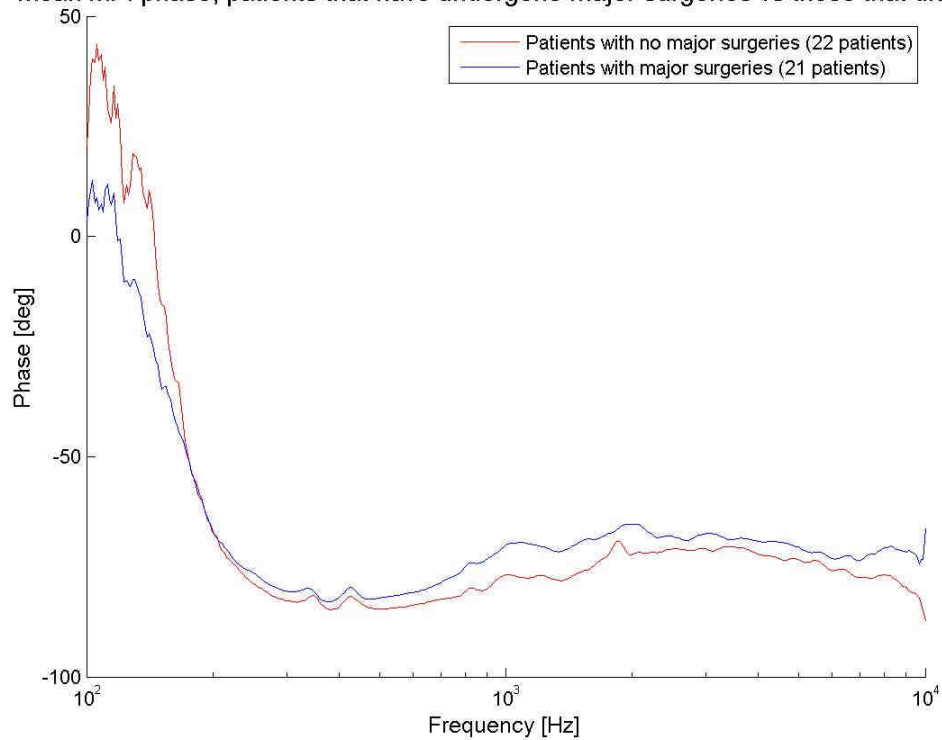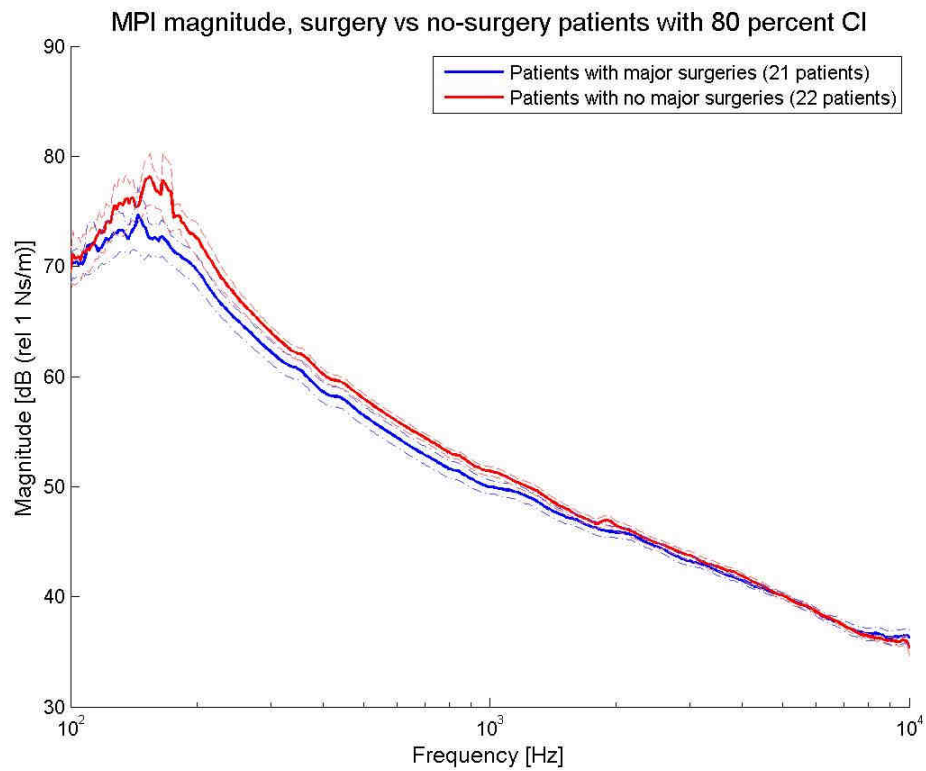**Figure 23 - Mean MPI magnitude of the patients that have undergone major ear surgeries vs those of patients that did not, with their 80% confidence intervals (dotted lines). (smoothed)**

Picture 24 shows an example of how the force frequency spectrum looks like; this particular is for patient number 18.
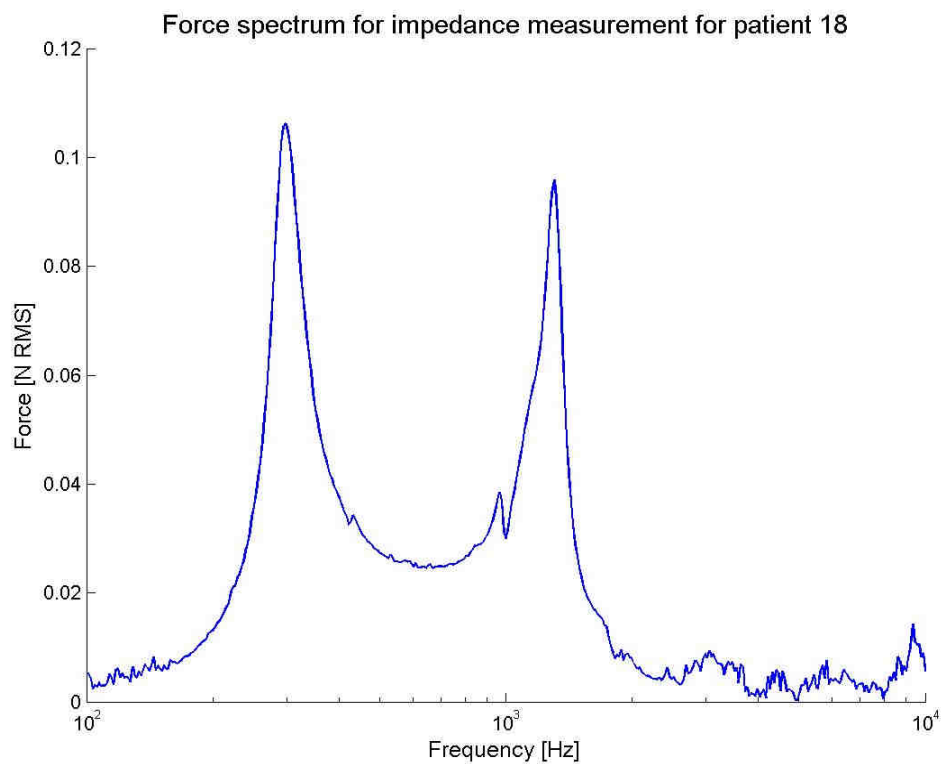
Figure 24 – Force frequency spectrum taken from MPI measurement on patient 18

Equivalence of the different measurement setups

In figure 25 the MPI of patients measured in Sweden was plotted against that of the patients measured in Canada. The idea was to evaluate the equivalence of both measurement setups and the approach taken was to look for major differences in their depicted means.
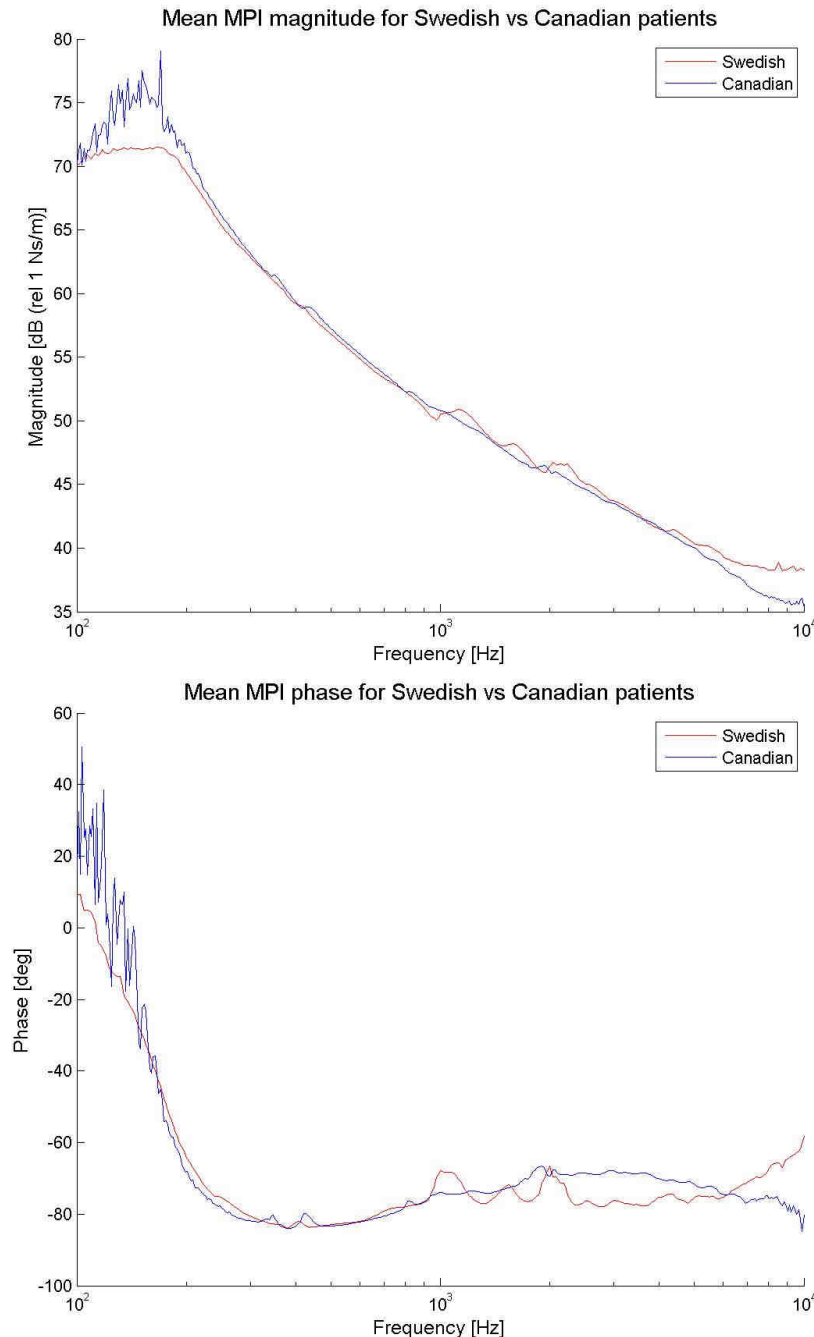
Figure 25 – Mean MPI magnitude and phase of Canadian vs Swedish patients. (smoothed)

Linearity

Patient 32 was randomly selected to be subject to linearity test measurements. Figure 26 shows patient 32's mechanical point impedance measured at 30, 40, and 50 dB relative to 1mN at 1 kHz.

Figure 26 – MPI magnitude and phase measured on patient 32 at three different excitation levels. (smoothed)

Coupling comparison test measurements

Picture 27 shows the mean mechanical point impedance magnitude and phase for the twelve patients whose abutment allowed for measurements using both Cochlear's traditional snap couplin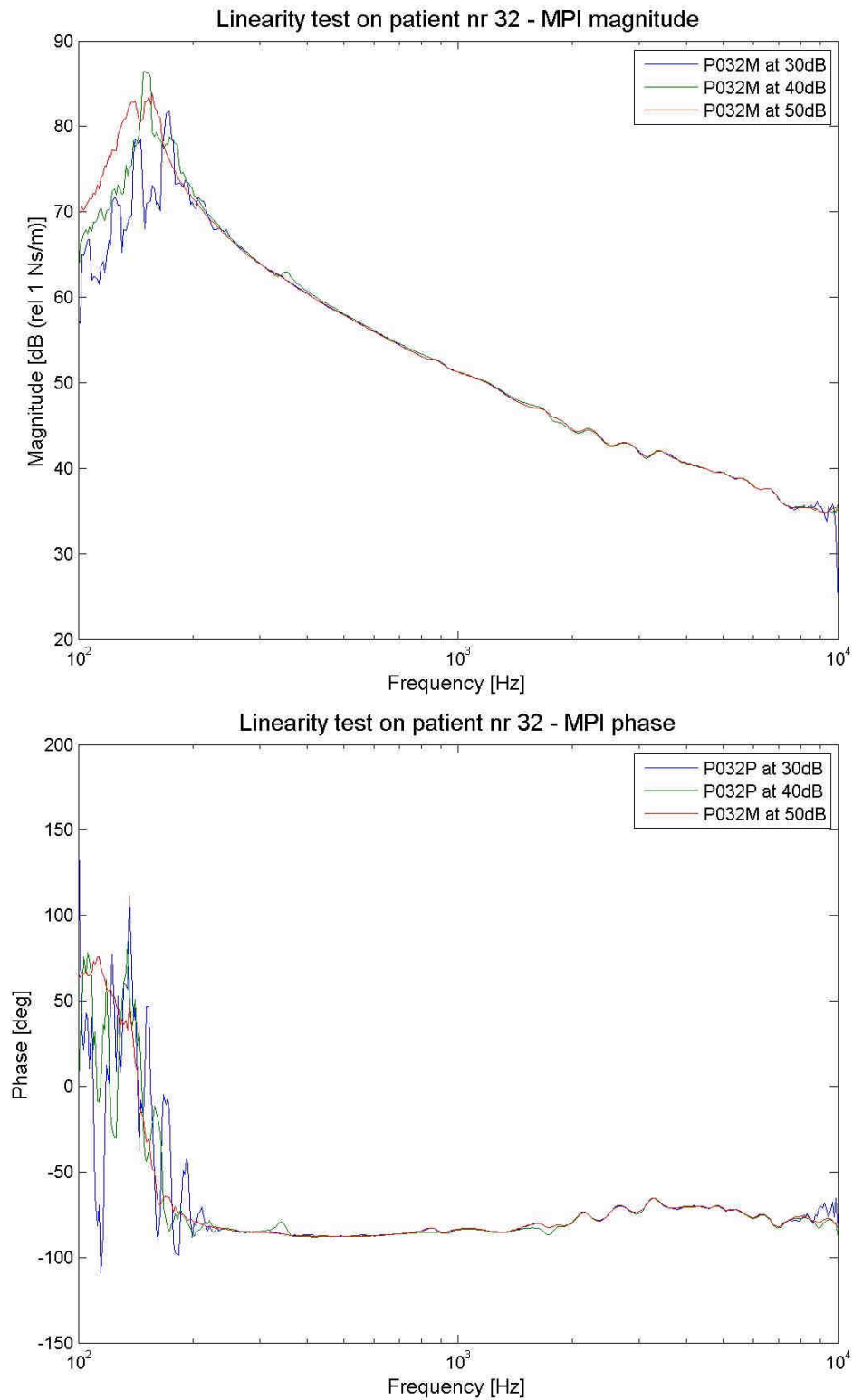g, as well as Oticon Medical's new coupling. Because of the difference observed in high frequencies, a new set of measurements was conducted on a skull simulator TU-1000 to try to determine the difference in their respective compliances.

Picture 28 shows the mean mechanical point impedance magnitude and phase for three consecutive measurements using each coupling on the skull simulator. Knowing that the internal mass of the skull simulator is of 55g, the difference in frequency at which the mass resonates with each compliance can be studied to investigate the difference in compliance. Reading the first antiresonance frequency from the graph, equation number 7 can be used to calculate the difference in compliance:

$$f_{antires} = \frac{1}{2 \cdot \pi \cdot \sqrt{m \cdot C}} \qquad (7)$$

Solving for C, each coupling's compliance value was determined, as shown in table 2.

Table 2 - compliance of the different couplings calculated from antiresonance analysis of MPI measurements

	Cochlear	Oticon
Antiresonance frequency [Hz]	1679	1567
Compliance value [n m/N]	163	187

Transfer function measurements

Due to programming problems, the transfer accelerance recordings made on five patients were considered unreliable. No pictures or results of this part are therefore presented in this report.

Figure 27 – MPI magnitude and phase of 12 patients measured with both couplings (dotted lines), and the means for the groups measured with each coupling (filled lines).
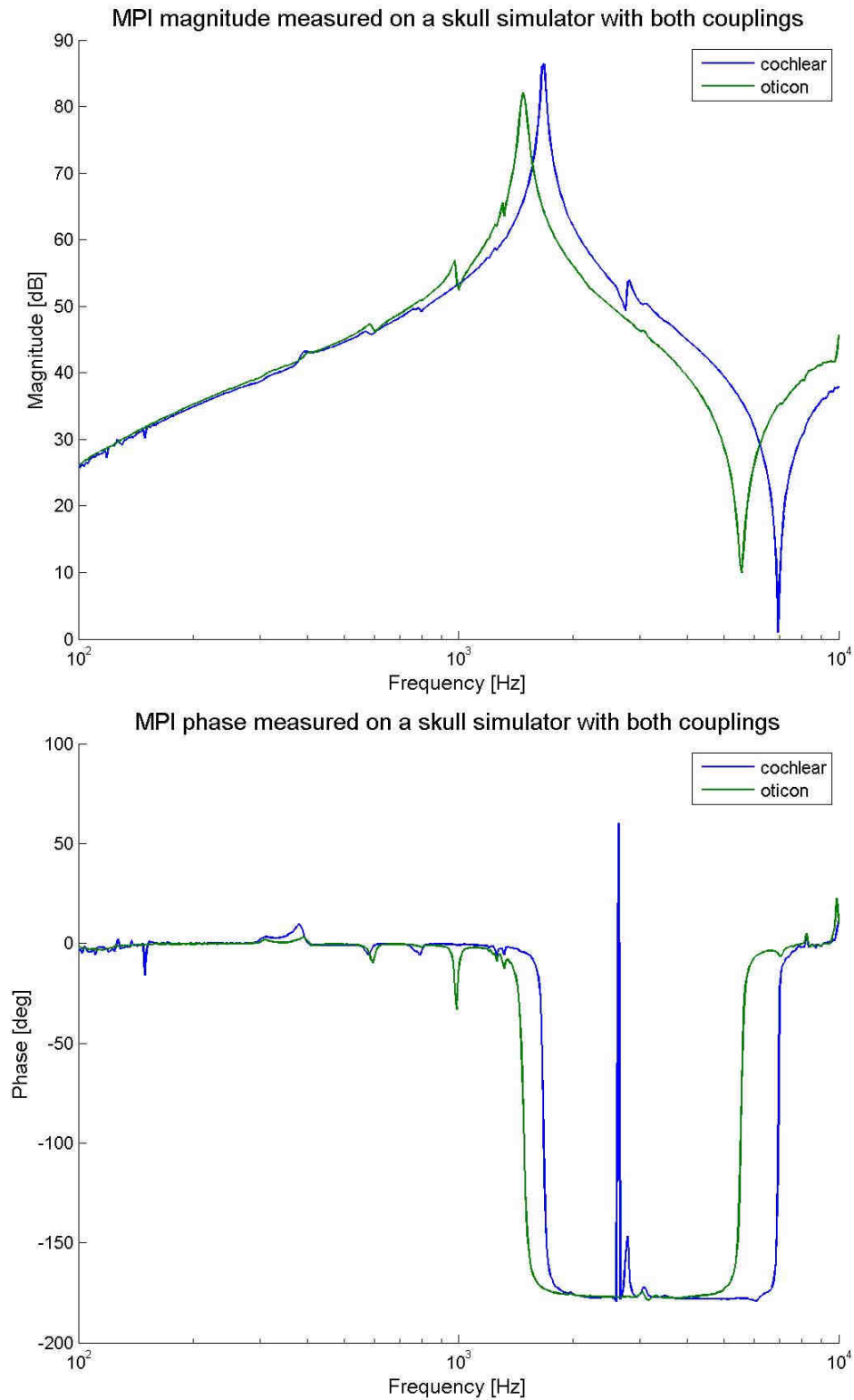
Figure 28 – Mean MPI magnitude and phase of three consecutive measurements with each coupling made on a TU-1000 skull simulator.

Modeling of mean MPI

Different modeling techniques were tested while pursuing a good mathematical model of the mean MPI. Table 3 shows the three models that achieved best fit. Table 4 in the appendix shows the rest of the produced models.

All three models presented below are second order models with one zero and two underdamped poles. The best model was the one lacking both delay and integrators, namely the one called P2ZU. This model achieved 89.2 percent fit, which means that it could explain 89.2% of the measured samples throughout the frequency range.
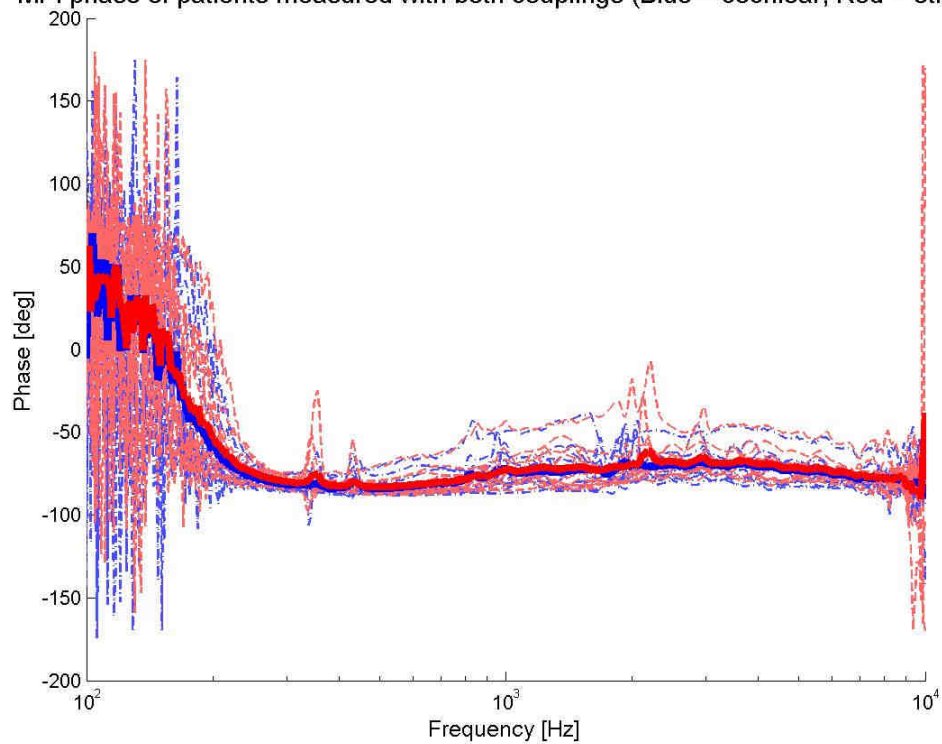
Table 3 - process models with best fit to the smoothed version of the mean MPI

| Name	Description	Parameters	Notes	%Fit to validation data
P2ZU	Process model with transfer function $$G(s) = Kp * \frac{1+Tz*s}{1+2*Zeta*Tw*s+(Tw*s)^2}$$	Kp = 1148.9 Tw = 0.0010615 Zeta = 0.24725 Tz = 0.0023799	Estimated using PEM using SearchMethod = Auto from data set z Loss function 665847 and FPE 674160	89.2
P2DZU	Process model with transfer function $$G(s) = Kp * \frac{1+Tz*s}{1+2*Zeta*Tw*s+(Tw*s)^2} * exp(-Td*s)$$	Kp = 1291.6 Tw = 0.0010534 Zeta = 0.23922 Td = 0 Tz = 0.0019841	Estimated using PEM using SearchMethod = Auto from data set z Loss function 38368.8 and FPE 38752.1	89.0
P2DIZU	Process model with transfer function $$G(s) = Kp * \frac{1+Tz*s}{s(1+2*Zeta*Tw*s+(Tw*s)^2)} * exp(-Td*s)$$	Kp = -2.409e+005 Tw = 0.001 Zeta = 0.25026 Td = 0 Tz = -0.0068872	Estimated using PEM using SearchMethod = Auto from data set z Loss function 48949.6 and FPE 49560.7	88.9
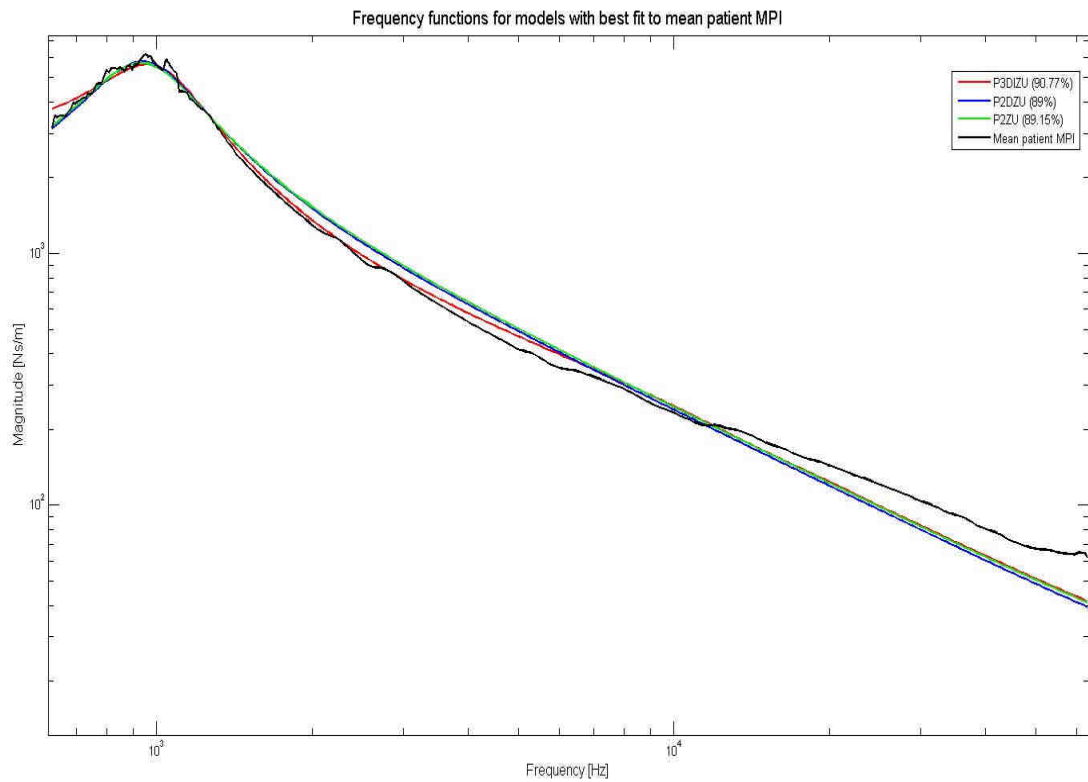
Figure 29 – Simulated MPI magnitude of three of the produced models, together with the smoothed mean measured MPI magnitude.

6.   Discussion

Mechanical impedance measurements

Previous studies by Stalnaker et al (1971) and Smith and Suggs (1976) show that there are no free resonances in the human skull below the frequency of 350Hz. For the measurements presented here it means that for every antiresonance present in that frequency range, the skull would not be able to show free oscillations after an impulse excitation. That being the case, these resonances don't belong to the structural properties of the skull. Such resonances are called "forced resonances", because they arise when a system is constantly fed with energy during the measurement.

Needless to say, the true mean of the whole population's MPI can, in practical terms, never be achieved because it would require measuring *every* patient. A statistical tool is therefore needed to estimate instead the accuracy of these measurements. The small relative size of the 95% confidence intervals around the mean mechanical point impedance for all measured patients depicted in figure 11 is a strong indicator that these measurements brought our understanding closer to the true population mean: the true population mean is with probability 0.95 within 2dB of the measured mean for low frequencies, and within 0.1 dB for higher frequencies.

Another important observation is that the confidence intervals around the mean impedance magnitude and phase are very close to the mean even for low frequencies, where the noise in the acceleration channel was at its highest level. This can only be possible if the amount of fluctuation above the mean is approximately the same size as that below the mean; which confirms that most of the artifacts found at low frequencies are due to randomized noise in the acceleration channel because of the low excitation levels chosen for the measurements, and not due to bias errors.

Comparing the shapes of the mean patient impedance with its confidence intervals vs. their smoothed version, we can see little or no difference throughout the frequency band apart for the disappearance of the noise spikes at low-frequencies. This proves that "smoothing" the mean impedance curves is a valid and useful tool to give the reader a better overview of the real impedance behavior underneath the measurements, without taking away any useful information.

Previous studies on live patients suggested a measure of the impedance magnitude that is very similar to what this study proposes as a very good estimator of the mean patient impedance. This is a very remarkable result, given the technology used in Håkansson's study from 1986, and the angle sensitivity of the coupling-abutment pair design used then. Similarities were also found with previous studies made on human cadavers; these latter ones can probably be regarded as good models of the mean patient MPI in vivo.

The impedance magnitude comparison between different groups of the patient pool revealed interesting results. The chosen confidence level was 80%, and the sample size is included in the legend of each figure. When comparing male vs. female patients, the differences observed in the frequency range 300 Hz – 2 kHz failed to prove statistically significant. The same was the case when the grouping factor was age, and patients were divided in above- and below the median

patient age of 49 years. In this last one, the sample size for the group of patients born between 1961 and 1993 was roughly half as big as that for those born between 1931 and 1961. The sample size directly affects the size of the confidence interval. In this case, the small sample size of the first group enlarged the confidence intervals around its mean but this was not the decisive factor as the means of both groups were too close to each other.

The same was the case in the comparison between patients with no known abnormalities in craniofacial anatomy vs. those patients with specific syndromes known to affect craniofacial anatomy,

A statistically significant difference in impedance magnitude was found in the frequency range 300 Hz – 600Hz when the older half of the patient pool was compared to the younger half. These results suggest that the impedance of the skull bone of older patients is around 2 dB (relative to 1 Ns/m) higher that that of younger patients in those frequencies; and also that with probability 0.8 there is a directly proportional relationship between age and impedance. What this means, is that the compliance in skull bone of older patients is harder than that of younger patients, which could be explained by the loss of calcium and other minerals in bone related to age. This also means that for the same force applied by a transducer, the skull bone of older patients would achieve a lower acceleration (less movement) which might need to be taken into consideration for prescriptive methods, and might also have an effect on battery consumption by the baha.

When comparing patients that have undergone major ear surgeries (group A) with those that didn't (group B), another statistically significant difference in MPI magnitude was found in the frequency range 220 Hz – 1100 Hz. The MPI magnitude for patients in group A was approximately 2 dB (relative to 1Ns/m) lower than that of the patients in group B. These results suggest that the impedance magnitude of the skull bone may be negatively affected by major surgeries; and also that with probability 0.8 there is an inverse proportional relationship between these two factors. What this could mean is that the compliance in skull bone of patients that have undergone major surgeries (group A) might have become softer after the surgical procedure. This also means that for the same force applied by a transducer, the skull bone of patients in group A would achieve a higher acceleration (more movement) which, again, might need to be taken into consideration for prescriptive methods, and might also have an effect on battery consumption by the baha.

The careful reader may notice that for this last comparison, the sample sizes do not add up to 45. The explanation is that surgery information was missing from three of the patients, so they could not be classified with regards to this factor.

These differences can be observed in a better way in figures 30 to 33, which are close-up pictures of figures 15, 18, 20 and 23 with zoom in the region of interest.

The low confidence level chosen for this specific study is a questionable factor: 1 out of 5 times, the relationship between impedance magnitude and the second studied factor could have been due to chance. At the same time, these studies were not part of the original plan for this research project. If they were, the patient pool would have been selected accordingly, so the confidence levels could be increased.
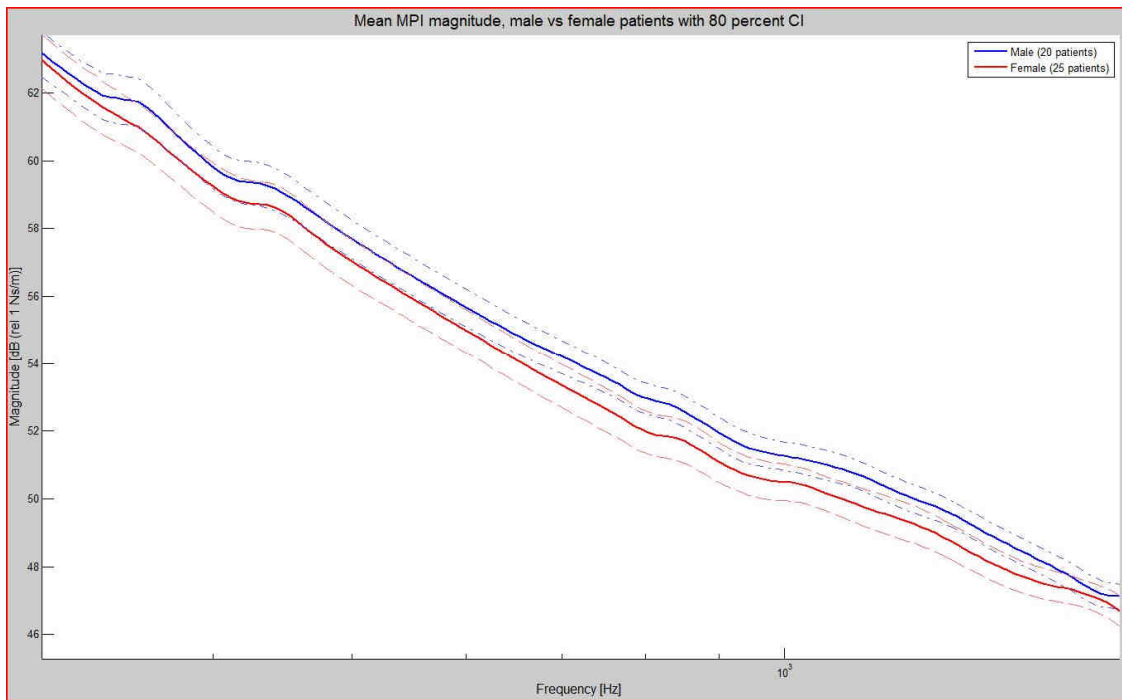
Figure 30 – closeup screenshot of mean MPI magnitude of male vs female patients, with their 80% confidence intervals showing only the frequencies of interest.
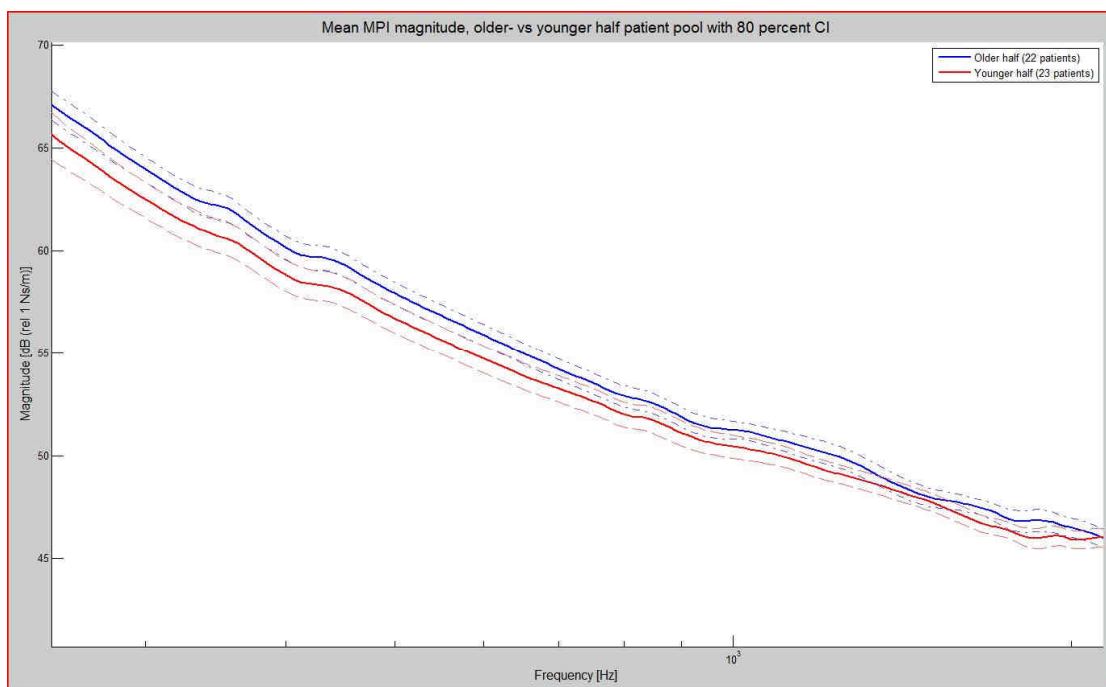
Figure 31 - closeup screenshot of mean MPI magnitude of older vs younger half of patient pool, with their 80% confidence intervals showing only the frequencies of interest.
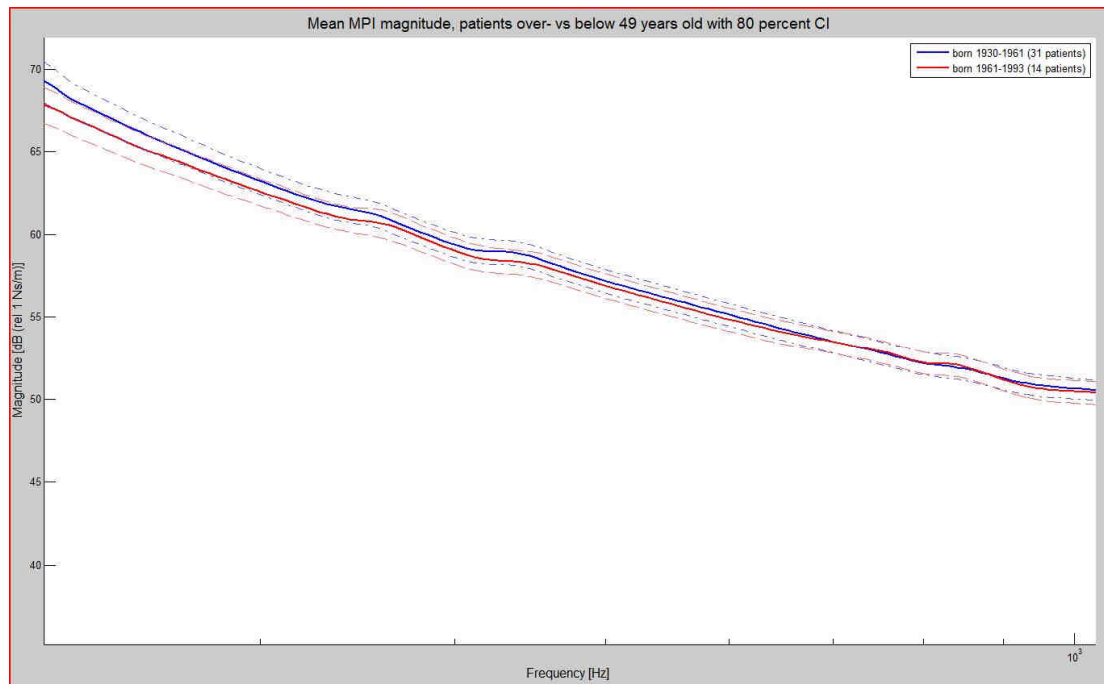
Figure 32 - closeup screenshot of mean MPI magnitude of patients above and below 49 years old, with their 80% confidence intervals showing only the frequencies of interest.

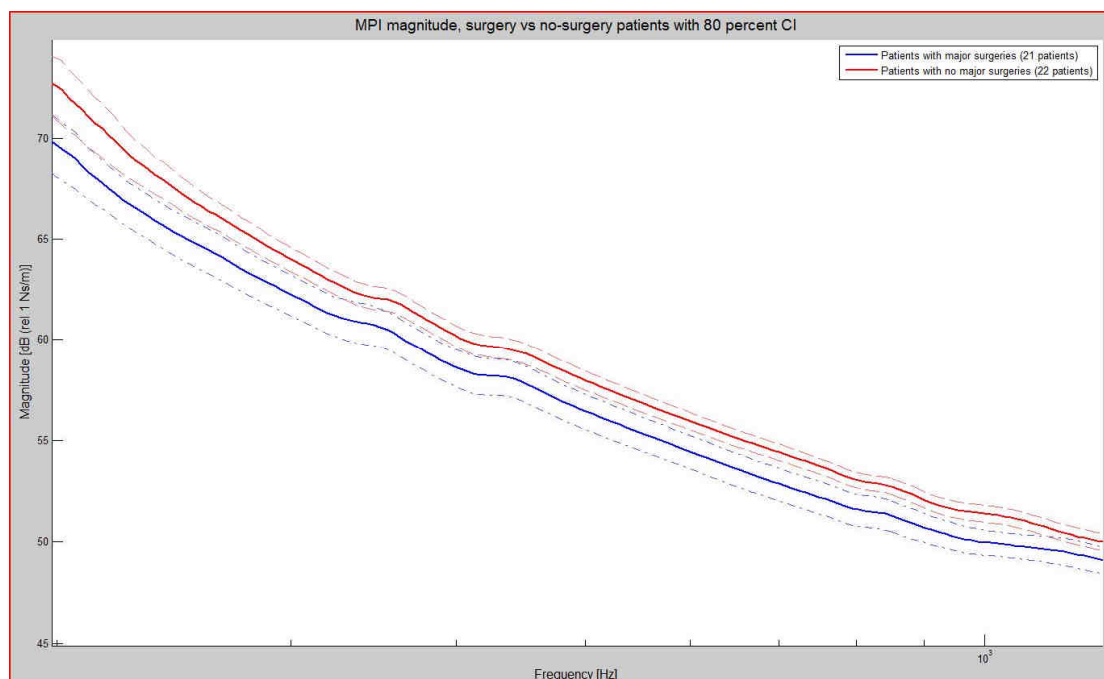**Figure 33 - closeup screenshot of mean MPI magnitude of patients with ear surgeries vs patients without, with their 80% confidence intervals showing only the frequencies of interest.**

The force output from the BEST transducer is frequency-dependent. It was calibrated to be 28.28 mN RMS at 1 kHz, which matches what can observed in figure 24.

Equivalence of the different measurement setups

The best way of studying the equivalence between measurement setups would be to measure the same patients with both setups, but it was not possible to do so in this study because of lack of resources. The approach taken is highly questionable because it does not give an estimate of the measurement difference in the same subjects but on different ones, and these are not directly comparable. At the same time, we now know that the MPI for most patients' skull lies within a certain range, and we can observe that so do both of the means in this specific result study in figure 25. It was then concluded that both measurement setups can be regarded as equivalent.

Linearity

Analyzing figure 26 it can be observed that, apart for the noise present in the lowest frequencies, the measured impedance is independent of the excitation level. It can then be assumed that the system is linear for the chosen excitation levels.

Coupling comparison test measurements

It can be observed in figure 27 that the magnitude measurements on patients are not noticeably affected in different ways by the use of either brand's couplings up to 2 kHz. This confirms what was expected from theoretical calculations: the compliance in the skull bone (around 400 m/N at 1 kHz) dominates the impedance behavior up to a certain frequency where it becomes too stiff and the coupling compliance starts dominating instead.

The measurements done with the skull simulator allowed for better understanding of these differences. Table 2 shows the calculated compliance value for both couplings. We can see that Oticon Medical's coupling is 15 % softer than Cochlear's coupling. The couplings used for this study were previously attached to test devices used very few times, and not to actual bahas used by patients. They can therefore be regarded as new so the wear and aging factors are minimal in both.

Above 2 kHz the impedance magnitude difference measured on patients is so small that it is unlikely that either of the coupling designs could negatively affect vibration transmission. However, a small shift in frequency for a specific resonance frequency in impedance measurements can generate big differences in the magnitude for the frequencies close to the resonance peak. These differences can significantly increase for impedance curves with steep slopes close to the resonance frequency.

For new couplings, the resonance frequency of Oticon's was proven to be lower than that for Cochlear's. On the other hand, the materials used for both couplings differ notably: Cochlear's is entirely made of plastic, which is known to wear with time and use. It is the author's opinion, that the difference in frequency for both couplings would be reversed with time, as Cochlear's coupling deteriorates and becomes softer.

It is known from own experimental measurements that a second impedance magnitude peak, caused an antiresonance between the coupling's mass and compliance, would be found if the measured range included higher frequencies. If the couplings actually became softer with time and use, these peaks could "move" towards lower frequencies and maybe be relocated at 8 – 9 kHz.

The author assumes the clinical importance of this to be minimal, as the hearing loss of most baha users impedes them from hearing such high frequencies.

No other work where the performance of the different coupling designs is compared has yet been published to this date. This is, as far as this author knows, the very first study of this kind in this field.

Transfer function measurements

Programming errors in the initial phases impeded this study from achieving good measurements of the transfer accelerance functions. At the same time, the major focus of the project was on the other goals and these measurements were regarded as of lesser importance. The patient pool was selected accordingly, which resulted in only five transfer function measurements were taken. The low sample size would probably fail in provide reliable generalizations by itself, disregarding the programming problems.

Modeling of mean MPI

The model that achieved best fit to the smoothed version of the mean MPI was a second order model, with one zero and two underdamped poles. This was expected from previous knowledge of second order mechanical systems.

Error estimation

Bias errors caused by impedance head of the design type used in this study have been comprehensively investigated in previous studies. It was found that such errors are negligible in measurements on the human skull (Håkansson and Carlsson, 1987).

The overall accuracy of the measurements made in this research project, with the selected methods and apparatus are dependent on several factors of which the following are likely to cause the most serious errors:
1. Calibration accuracy of gain factors of the different sensors
2. Imperfect mass compensation, mainly from measurements of the different masses
3. Interaction of the piezoelectric load cell's compliance used for force measurement with the measured impedance
4. Noise in the acceleration channel due to low excitation level.

Factor number 1 could affect the measurements throughout the whole frequency band. Factors number 3 and 4 are most likely to influence the impedance behavior at low frequencies, whereas the impact from issue number 2 can mostly be seen at higher frequencies. To estimate what kind of effect these uncertainty factors may have on the overall impedance behavior, their nature needs to

be taken into account and their size needs to be compared relative to the measured impedance at different frequencies. The sizes of some factors are easier to estimate than for others.

The amount of noise in the acceleration channel signal could have been reduced considerably by choosing a higher excitation level for the transducer during the swept sine measurement. This being an *in vivo* study, that possibility had to be discarded to avoid patient discomfort.

Measurement procedure

There is no given or well-known way of perform this kind of measurements. Therefore, what is needed is to perform tests towards an acceptable measurement procedure. An important part of this testing was to decide whether allowing the patient to sit in an upright position would negatively affect the measurement outcome, being this position otherwise very convenient because it saves time and it is more natural for the patient.

To ask the patient to lie down on a bed during the measurement could lead to the problem of how to support the patient's head in order to avoid getting the bed's structure characteristics in the vibration measurements. This is not a problem when it comes to the rest of the patient's body being in contact with some other structure, because the head and the body's vibration characteristics are mechanically disconnected by the compliance in the soft tissues of the neck.

The differences observed in the measurements when changing the angle of the head were in the order of 1 dB and not even noticeable for some angles.

Intersubject variations

The observed intersubject variations can originate from different sources. Skull bone thickness at the implant's host site is a highly variable factor that can directly affect the shearing strength of that bone. Other skull bone characteristics like mass and elasticity module could also have a significant effect on the measured impedance.

During patient measurements it was also noticed that the implant's angle relative to the skull bone surface could significantly vary from patient to patient. There are standards for the implant's location and angle, but ultimately these are decided by the surgeon at the time of the procedure. The variability of this factor should be minimal, but this was not the case. The angle of the implant directly affects the excitation angle at the time of the measurement. Different excitation angles can generate different bending modes in the skull, which can affect the measured impedance.

Intrasubject variations

Intrasubject variations were only studied in patient 32 as a side study of the linearity test. The different measurements were taken within some minutes from each other. Disregarding the low frequency noise, the biggest differences are for frequencies between 200 Hz and 300 Hz. These

differences are within 1 dB relative to 1 Ns/m, which represents 1.5% of the mean measured impedance at that specific frequency point.

The small amount of time between each of the measurements for this test is a questionable factor and should be considered for future studies.

7.   Conclusions

The first observation to be made is that the existing measurement setup at the department of Signals and systems of Chalmers University of Technology, and the setup designed, programmed and built for this project at the Interfacial Biomechanics Laboratory at iRSM are equivalent. Their measurements are therefore comparable.

The test made to prove the linearity of the abutment-skull system was positive. The system is then assumed linear for the chosen excitation levels.

Quick observations of the results obtained in this project indicate that they are very similar to those obtained by Håkansson in 1986. The mean frequency for the first forced antiresonance was found to be 147 Hz as opposed to the 145 Hz proposed by Håkansson. The similarities observed while comparing these results to those obtained from measurements in human cadavers, is that these latter ones are good models of the mechanical point impedance of the human skull in vivo.

The spread observed in figure 10 indicates that the impedance magnitude for most patients lie within a 4 dB range for most of the measured frequencies. However, a few outliers can be observed, whose impedance magnitude is around 10 dB lower than the rest. For these patients, 10 dB less impedance mean 10 dB more acceleration than the rest of the patients, and thus 10 times more movement in the measured region for the same applied force. This fact doesn't affect the general impedance mean in a visible way, but for those specific patients this 10 dB difference could be of clinical importance.

The true population mean is with probability 0.95 within 2dB of the measured mean for low frequencies, and within 0.1 dB for higher frequencies.

The analysis and comparison of the mechanical properties of the couplings manufactured by Oticon medical and Cochlear revealed that the first ones are 15% softer than the latter ones when they are new. Nevertheless, both couplings are considered to be sufficiently stiff to be able to transmit vibrations without negatively affecting this process. Analysis of the materials used for each let the author speculate about the possible reversal of this relationship with continuous use of both over time, as the plastic material used for Cochlear's coupling is more prone to wear with time.

The comparative tests of patient groups based on a certain patient parameter or the absence of it indicate statistically significant differences in MPI at 80%, in certain frequencies, in two of the comparisons, namely "older- vs. younger half patient pool", and "patients with major ear surgeries vs. patients without". Older patients show a tendency towards higher skull impedance in the frequency region 300 Hz to 600 Hz compared to younger patients. Patients that have undergone major ear surgeries show lower skull impedance (softer skull compliance) in the frequency range 200 Hz – 1.2 kHz than patients whose skull has never been exposed to such a procedure.

This study did not find statistically significant differences in MPI in two of the other studied comparisons, namely "patients with no known abnormalities in skull anatomy vs. patients with specific syndromes known to affect craniofacial anatomy" and "male patients vs. female patients".

8.   Future work

Future work in this field should focus on different patient groups, for example pediatric patients. It would also be interesting to investigate the effect of new parameters on the MPI, in particular those parameters that are easily measurable on patients without implants, and that could give a reliable estimate of the patients MPI prior to the surgical implantation.

Also, it would be interesting to study the effects of aging and use on both couplings over a long period of time. Finally, a new study of transfer accelerance function that addresses the difficulties encountered in this study needs to be made.

9.   References

Albrektsson, T., Brånemark, P.-I., Hansson, H.-A., Kasemo, B., Larsson, K., Lundström, I ., McQueen, D., and Skalak, R. (1983). "The interface zone of inorganic implants in vivo: Titanium implants in bone", Ann, Biomed. Eng. 11, 1-27.

Brånemark, P.I., Hansson, B.-O., Adell, R., Breine, U. Lindström, J., Hallén, O., and Öhman, A. (1977). "Osseointegrated implants in the treatment of the edentulous jaw", Scand. J. Plast. Reconstr. Surg. 11, Suppl. 16.

Carlsson, P., Håkansson, B. and Ringdahl, A., (1995) "Force threshold for hearing by direct bone conduction", J. Acoust. Soc. Am. 97(2), 1124-1129.

Håkansson, B., Carlsson, P., and Tjellström, A. (1986). "The mechanical point impedance of the human head with and without skin penetration", J. Acoust. Soc. Am. 80(4), 1065-1075.

Håkansson, B., and Carlsson, P. (1987)." Bias errors in mechanical impedance data obtained with impedance heads", J. Sound Vib. 113(1).

Smith, J. B., and Suggs, C. W., (1976). "Dynamic properties of the human head," J. Sound Vib. 48(1), 35-43.

Stalnaker, R. L., Fogle, J. L., and McElhaney, J. H. (1971). "Driving point impedance characteristics of the head," J. Biomech. 4, 127-139.

WHO Fact sheet N°300 (2010) World Health Organizati on, Available: http://www.who.int/mediacentre/factsheets/fs300/en/index.html Last accessed: 27th March, 2011

10. APPENDIX

Other mathematical models of MPI

Table 4 - other produced models for mean MPI

Name	Description	Parameters	Notes	%Fit to validation data
P3U	Process model with transfer function $$G(s) = \frac{Kp}{(1+2*Zeta*Tw*s+(Tw*s)^2)(1+Tp3*s)}$$	Kp = -3.1253e+005 Tw = 0.0011588 Zeta = 0.3526 Tp3 = 0.11301	Estimated using PEM using SearchMethod = Auto from data set z Loss function 1.13897e+006 and FPE 1.15035e+006	**78.21**
P2DIU	Process model with transfer function $$G(s) = \frac{Kp}{s(1+2*Zeta*Tw*s+(Tw*s)^2)} * exp(-Td*s)$$	Kp = -2.8997e+006 Tw = 0.001 Zeta = 0.3893 Td = 0.00058594	Estimated using PEM using SearchMethod = Auto from data set z Loss function 707074 and FPE 714135	**79.17**
P2IZU	Process model with transfer function $$G(s) = Kp * \frac{1+Tz*s}{s(1+2*Zeta*Tw*s+(Tw*s)^2)}$$	Kp = -1.9726e+006 Tw = 0.001 Zeta = 0.34 Tz = -0.0010879	Estimated using PEM using SearchMethod = Auto from data set z Loss function 627646 and FPE 633914	**83.81**
P2U	Process model with transfer function $$G(s) = \frac{Kp}{1+2*Zeta*Tw*s+(Tw*s)^2}$$	Kp = 1237.6 Tw = 0.001 Zeta = 0.21474	Estimated using PEM using SearchMethod = Auto from data set z Loss function 2.95305e+006 and FPE 2.97517e+006	**84.81**
P3DU	Process model with transfer function $$G(s) = \frac{Kp}{(1+2*Zeta*Tw*s+(Tw*s)^2)(1+Tp3*s)} * exp(-Td*s)$$	Kp = -5.8544e+005 Tw = 0.001 Zeta = 0.32299 Tp3 = 0.21762 Td = 0.00057609	Estimated using PEM using SearchMethod = Auto from data set z Loss function 665847 and FPE 674160	**85.46**
P2DU	Process model with transfer function $$G(s) = \frac{Kp}{1+2*Zeta*Tw*s+(Tw*s)^2} * exp(-Td*s)$$	Kp = 1246.6 Tw = 0.001 Zeta = 0.23626 Td = 0	Estimated using PEM using SearchMethod = Auto from data set z Loss function 2.99358e+006 and FPE 3.02347e+006	**86.13**
P3ZU	Process model with transfer function $$G(s) = Kp * \frac{1+Tz*s}{(1+2*Zeta*Tw*s+(Tw*s)^2)(1+Tp3*s)}$$	Kp = 1288.7 Tw = 0.001 Zeta = 0.23962 Tp3 = 0.001 Tz = 0.0021603	Estimated using PEM using SearchMethod = Auto from data set z Loss function 1.66053e+006 and FPE 1.68126e+006	**86.22**
P3DZU	Process model with transfer function $$G(s) = Kp * \frac{1+Tz*s}{(1+2*Zeta*Tw*s+(Tw*s)^2)(1+Tp3*s)} * exp(-Td*s)$$	Kp = 1239.4 Tw = 0.001 Zeta = 0.24281 Tp3 = 0.001 Td = 0 Tz = 0.002336	Estimated using PEM using SearchMethod = Auto from data set z Loss function 1.55696e+006 and FPE 1.58028e+006	**86.28**
P3IZU	Process model with transfer function $$G(s) = Kp * \frac{1+Tz*s}{s(1+2*Zeta*Tw*s+(Tw*s)^2)(1+Tp3*s)}$$	Kp = -3.7511e+006 Tw = 0.001 Zeta = 0.28279 Tp3 = 0.00144 Tz = 0.00018064	Estimated using PEM using SearchMethod = Auto from data set z Loss function 943119 and FPE 954893	**88.49**

Patient database

Table 5 –Part of the patient database

Pat Number	Measured side	Gender	Date of Birth
P001	R	male	1950-02-16
P002	both	female	1936-08-01
P003	both	female	1954-10-08
P004	L	male	1950-12-23
P005	L	female	1940-07-11
P006	L	male	1946-03-01
P007	L	female	1939-06-17
P008	R	male	1940-03-13
P009	L	male	1967-08-12
P010	R	female	1944-08-13
P011	both	male	1953-02-25
P012	R	female	1975-11-26
P013	R	female	1986-09-12
P014	R	male	1979-09-09
P015	L	male	1948-09-07
P016	R	female	1971-06-24
P017	L	female	1952-04-13
P018	L	male	1947-03-06
P020	L	female	1955-04-18
P021	L	female	1970-10-15
P023	R	female	1936-01-12
P024	R	male	1961-05-07
P025	both	male	1965-10-31
P026	R	female	1956-05-10
P027	R	female	1950-11-04
P028	both	male	1949-09-08
P029	both	male	1988-05-22
P030	L	male	1967-01-26
P031	R	male	1937-09-10
P032	L	male	1942-02-12
P033	R	female	1975-10-02
P034	L	female	1931-12-18
P035	R	male	1945-10-30
P036	R	female	1949-08-05
P037	R	female	1941-10-21
P038	R	female	1945-01-12
P039	R	female	1960-08-22
P040	R	male	1983-01-06
P041	L	female	1949-04-10
P042	L	female	1958-04-09
P043	L	female	1941-07-12
P044	R	female	1977-03-18
P045	R	male	1943-03-22
P046	R	female	1993-04-29
P047	R	male	1961-06-06

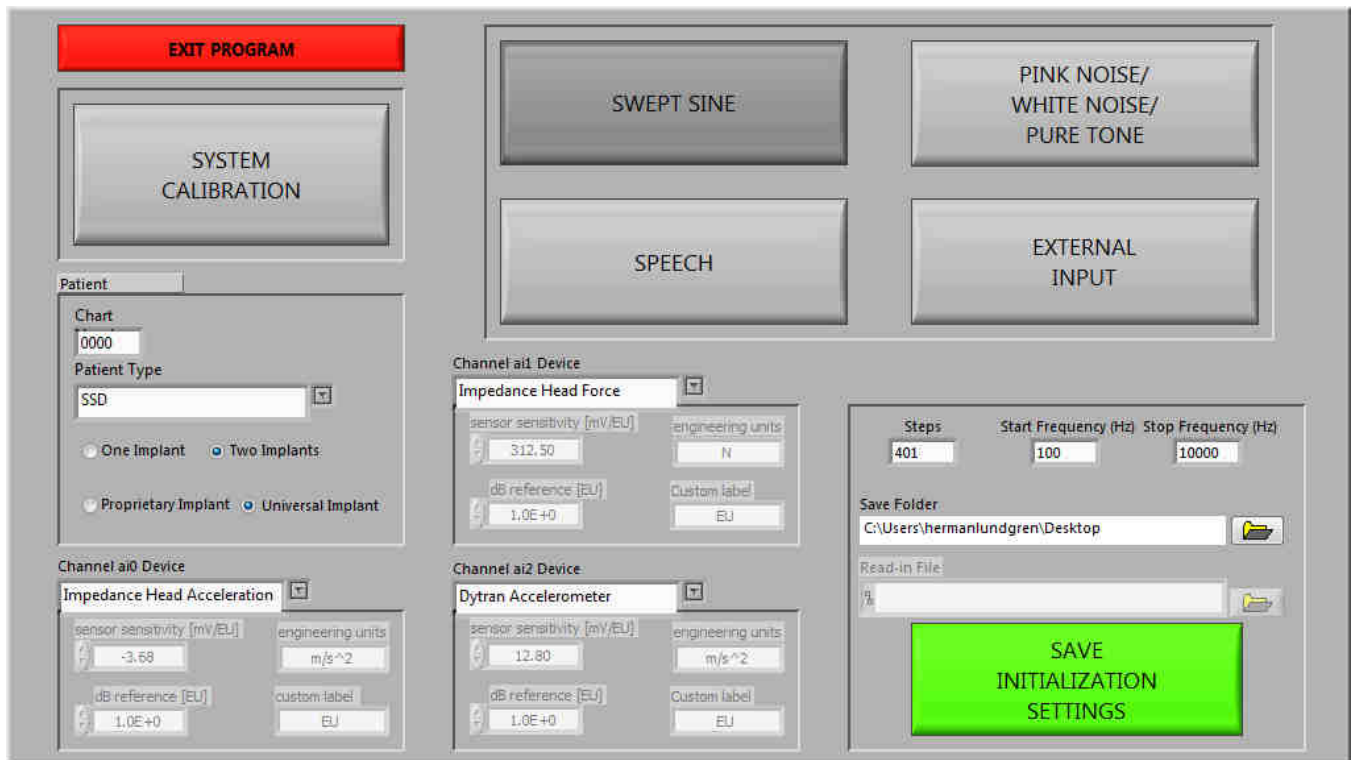# Virtual instrument for MPI measurements in Canada

Figure 34 – screenshot of the LabView program's graphical interface
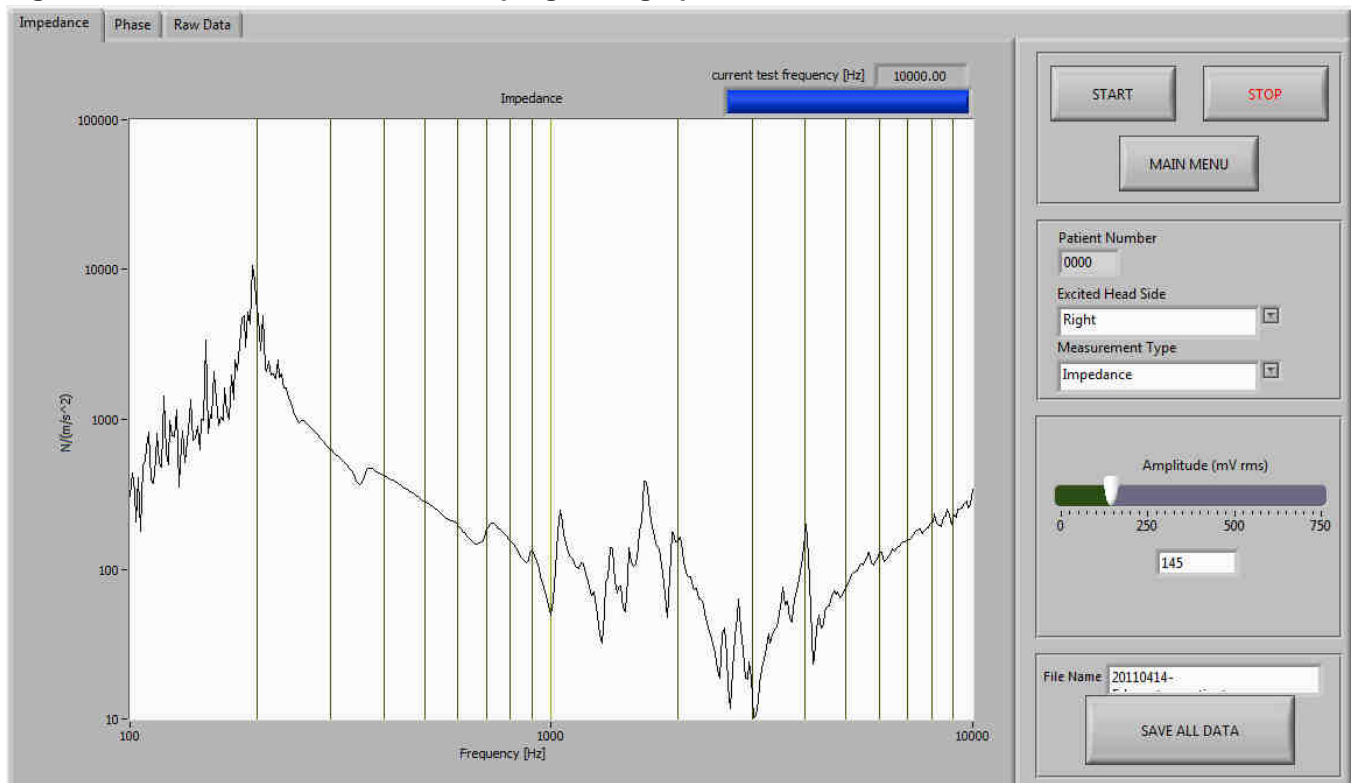

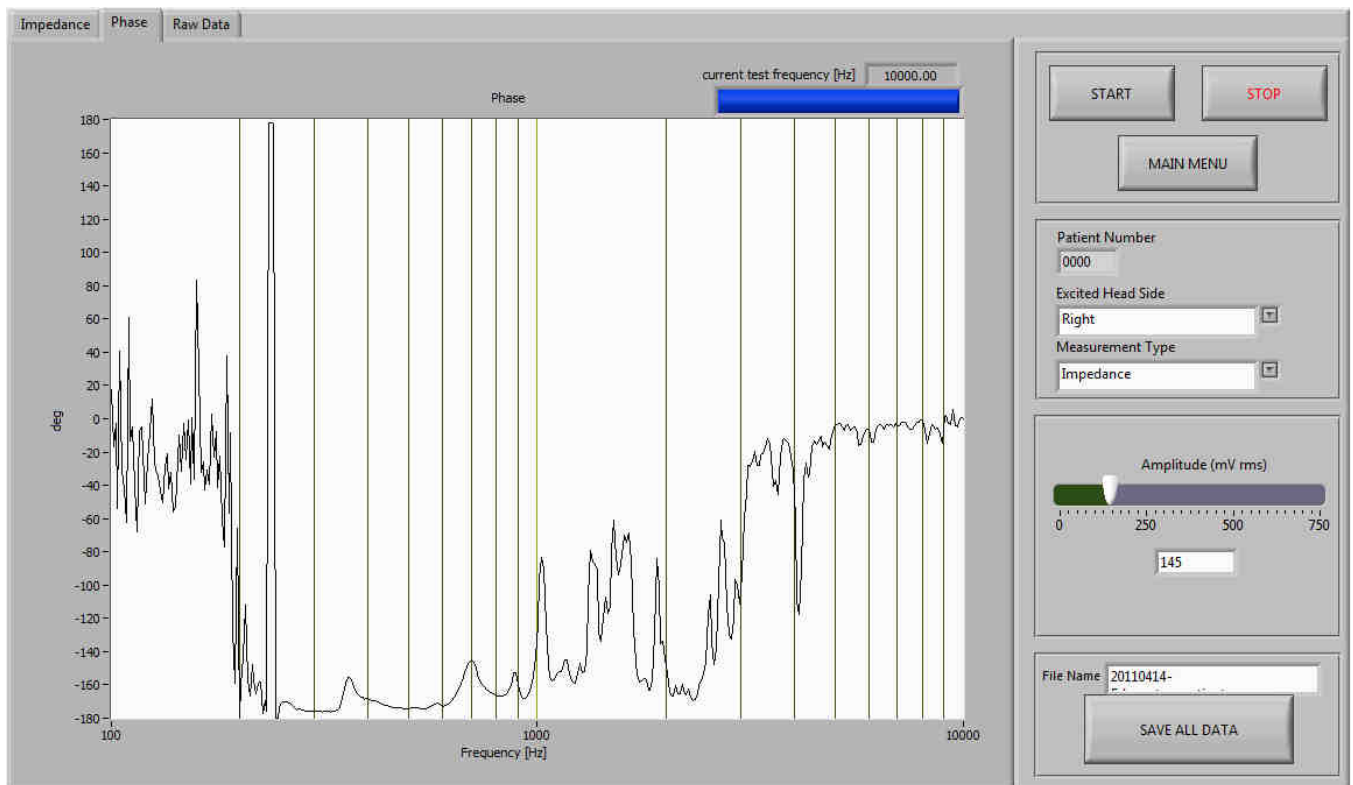**Figure 35 - screenshot of the LabView program's graphical interface**

Figure 36 - screenshot of the LabView program's graphical interface
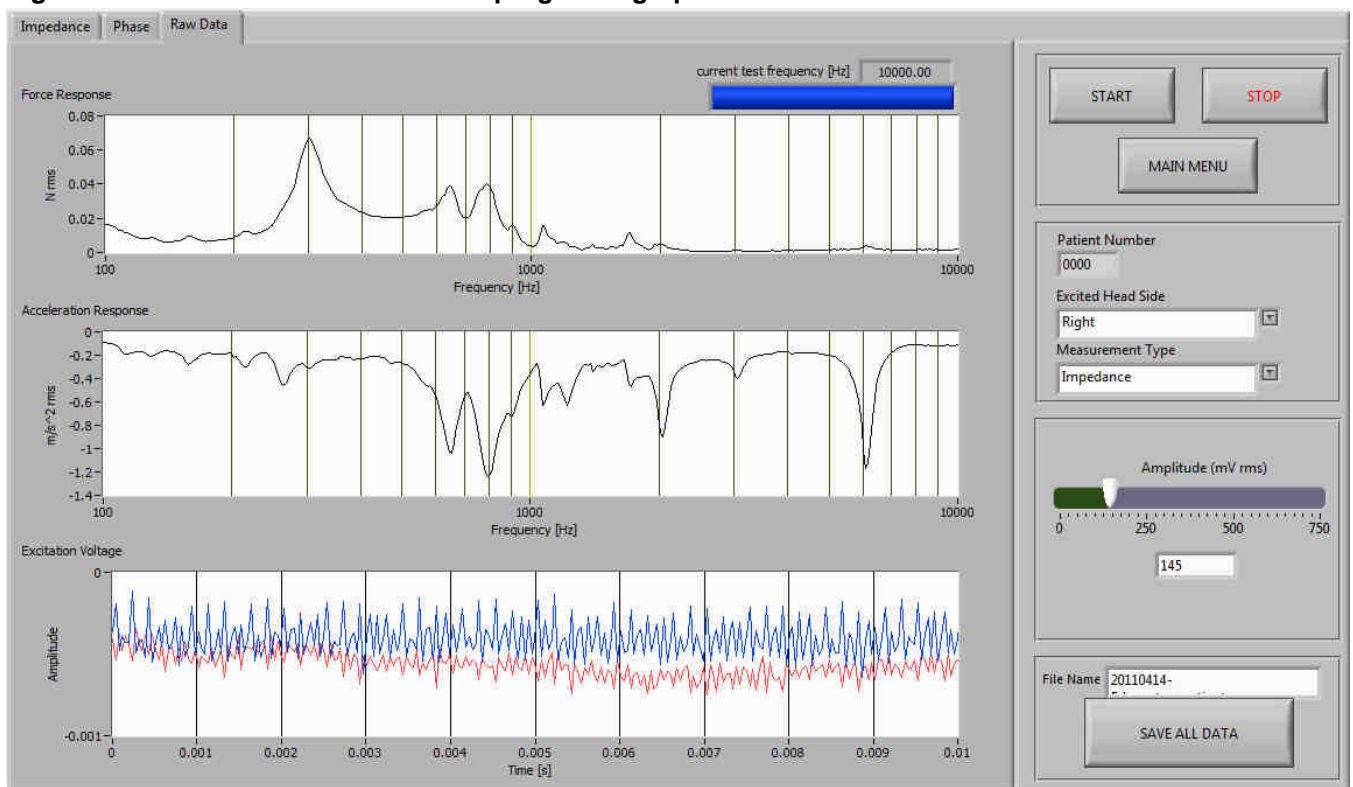

Figure 37 - screenshot of the LabView program's graphical interface
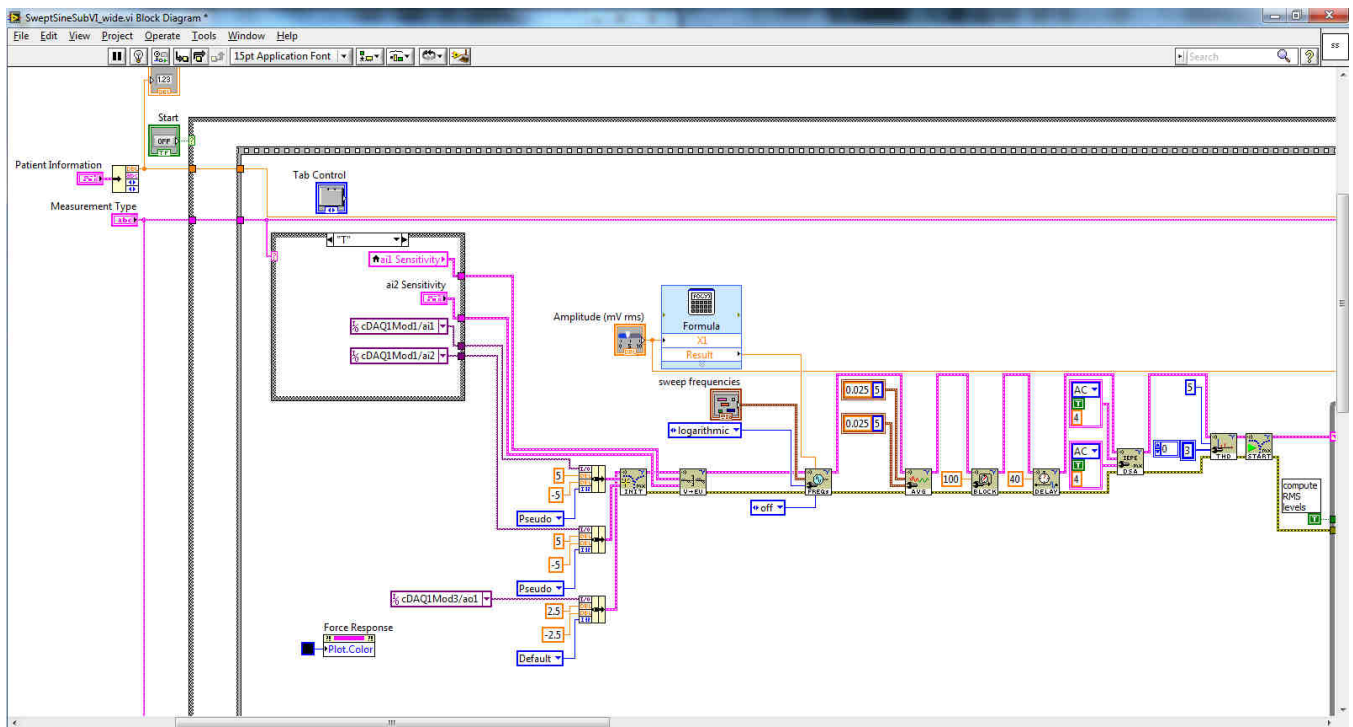
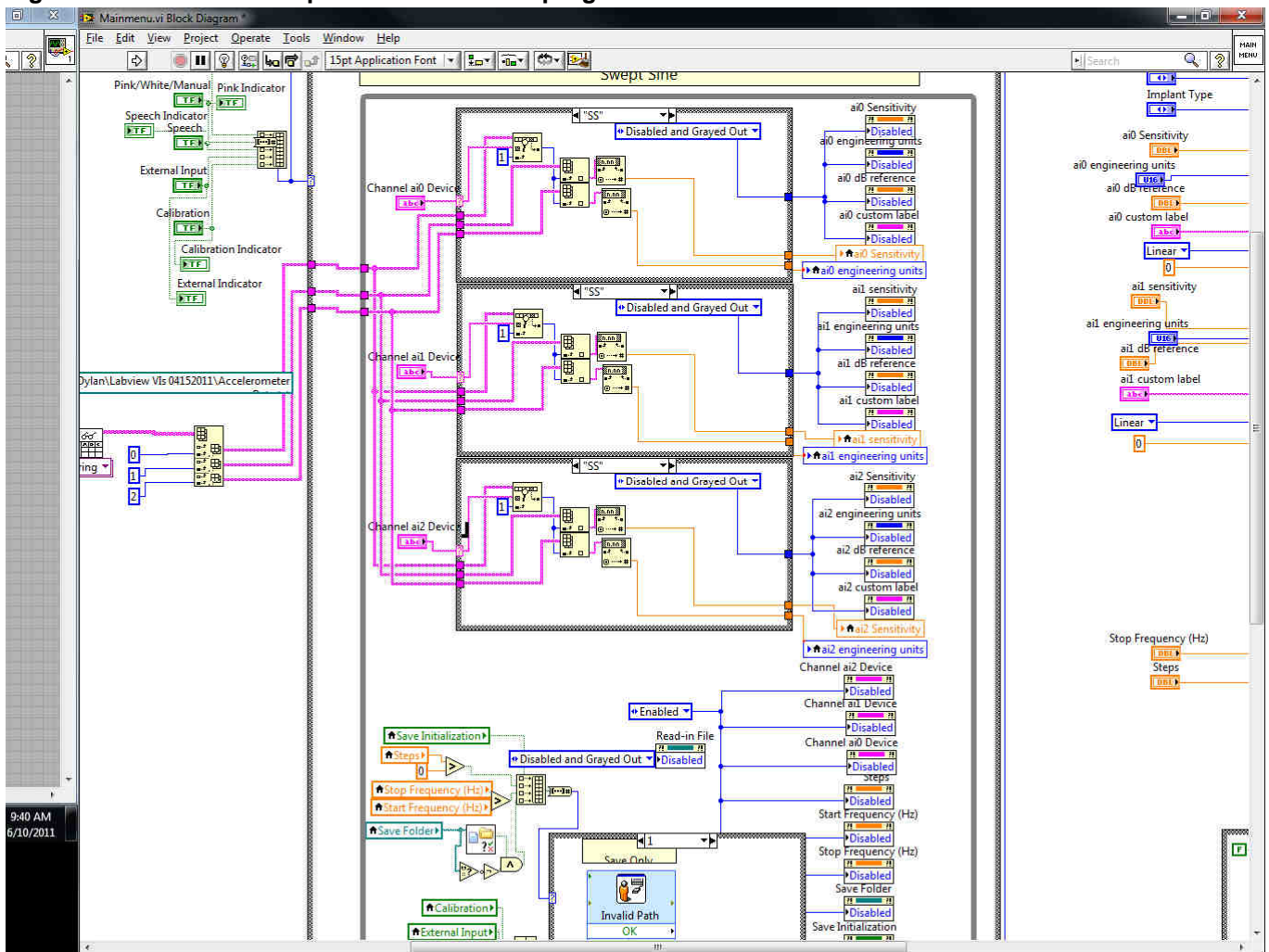**Figure 38 - screenshot of part of the LabView program's source code**

Figure 39 - screenshot of part of the LabView program's source code

Figure 40 - screenshot of part of the LabView program's source code